


RESEARCH

Open Access



Repeated intrathecal injections of peripheral nerve-derived stem cell spheroids improve outcomes in a rat model of traumatic brain injury

Hae Eun Shin^{1†}, Won-Jin Lee^{2,3†}, Kwang-Sook Park^{4,5†}, Yerin Yu¹, Gyubin Kim¹, Eun Ji Roh¹, Byeong Gwan Song¹, Joon-Hyuk Jung¹, Kwangrae Cho³, Young-hu Ha^{2,6}, Young-Il Yang^{2,6*} and Inbo Han^{4,5*} 

Abstract

Background Traumatic brain injury (TBI) is a major cause of disability and mortality worldwide. However, existing treatments still face numerous clinical challenges. Building on our prior research showing peripheral nerve-derived stem cell (PNSC) spheroids with Schwann cell-like phenotypes can secrete neurotrophic factors to aid in neural tissue regeneration, we hypothesized that repeated intrathecal injections of PNSC spheroids would improve the delivery of neurotrophic factors, thereby facilitating the restoration of neurological function and brain tissue repair post-TBI.

Methods We generated PNSC spheroids from human peripheral nerve tissue using suspension culture techniques. These spheroids were characterized using flow cytometry, immunofluorescence, and reverse-transcription polymerase chain reaction. The conditioned media were evaluated in SH-SY5Y and RAW264.7 cell lines to assess their effects on neurogenesis and inflammation. To simulate TBI, we established a controlled cortical impact (CCI) model in rats. The animals were administered intrathecal injections of PNSC spheroids on three occasions, with each injection spaced at a 3-day interval. Recovery of sensory and motor function was assessed using the modified neurological severity score (mNSS) and rotarod tests, while histological (hematoxylin and eosin, Luxol fast blue staining) and T2-weighted magnetic resonance imaging analyses, alongside immunofluorescence, were conducted to evaluate the recovery of neural structures and pathophysiology.

Results PNSC spheroids expressed high levels of Schwann cell markers and neurotrophic factors, such as neurotrophin-3 and Ephrin B3. Their conditioned medium was found to promote neurite outgrowth, reduce reactive oxygen species-mediated cell death and inflammation, and influence M1-M2 macrophage polarization. In the CCI rat model, rats receiving repeated triple intrathecal injections of PNSC spheroids showed significant improvements

[†]Hae-Eun Shin, Won-Jin Lee and Kwang-Sook Park contributed equally to this work.

*Correspondence:
Young-Il Yang
yang.youngil@gmail.com
Inbo Han
hanib@cha.ac.kr

Full list of author information is available at the end of the article



© The Author(s) 2024. **Open Access** This article is licensed under a Creative Commons Attribution-NonCommercial-NoDerivatives 4.0 International License, which permits any non-commercial use, sharing, distribution and reproduction in any medium or format, as long as you give appropriate credit to the original author(s) and the source, provide a link to the Creative Commons licence, and indicate if you modified the licensed material. You do not have permission under this licence to share adapted material derived from this article or parts of it. The images or other third party material in this article are included in the article's Creative Commons licence, unless indicated otherwise in a credit line to the material. If material is not included in the article's Creative Commons licence and your intended use is not permitted by statutory regulation or exceeds the permitted use, you will need to obtain permission directly from the copyright holder. To view a copy of this licence, visit <http://creativecommons.org/licenses/by-nc-nd/4.0/>.

in sensory and motor function, with considerable neural tissue recovery in damaged areas. Notably, this treatment promoted nerve regeneration, axon regrowth, and remyelination. It also reduced glial scar formation and inflammation, while encouraging angiogenesis.

Conclusion Our findings suggest that repeated intrathecal injections of PNSC spheroids can significantly enhance neural recovery after TBI. This effect is mediated by the diverse neurotrophic factors secreted by PNSC spheroids. Thus, the strategy of combining therapeutic cell delivery with multiple intrathecal injections holds promise as a novel clinical treatment for TBI recovery.

Keywords Traumatic brain injury, Peripheral nerve-derived stem cells, Spheroids, Intrathecal injection, Neuroregeneration, Functional recovery, Neurotrophic factor

Introduction

Traumatic brain injury (TBI) represents a significant global health concern, as it is a major cause of mortality and long-term disability in various demographics groups. TBI can result from a variety of incidents, resulting in extensive and complex brain damage. This damage typically presents as a mix of localized lesions and diffuse brain injuries, which together lead to a range of physical, cognitive, and behavioral deficits [1, 2]. Despite advances in understanding the underlying mechanisms of TBI, the medical community still faces challenges in finding effective treatments that substantially improve patient outcomes in terms of survival and neurological recovery. To date, current therapeutic strategies have not provided a definitive solution for reducing mortality or alleviating the neurological impairments associated with TBI [3].

In the quest to improve the outcomes of TBI treatment, researchers are exploring a range of innovative therapies. Stem cell therapy and gene therapy are particularly notable for their potential to rehabilitate neurological functions in affected individuals [4, 5]. Although over 1,400 interventional trials for TBI treatments are registered on ClinicalTrials.gov, only 16 of these have investigated stem cell applications. Of this small subset, results from just 12 trials have been published. A common approach in these studies involves administering a single dose of autologous bone marrow mononuclear or mesenchymal stem cells to patients with chronic and severe TBI [6]. Research into TBI treatment has also explored the use of adipose-derived stromal vascular fraction [7], umbilical cord stem cells [8], and genetically engineered stem cells (SB623) [9]. A phase II trial using SB623 for chronic TBI patients has been completed, showing significant improvements in motor abilities [9, 10]. These encouraging results have prompted the filing for FDA approval in Japan. However, despite the regenerative potential demonstrated by SB623, challenges remain, including the need for repeated plasmid DNA transfections and additional interventions at the site of the infarct.

In our previous work, we successfully developed spheroids from human allogeneic peripheral nerve-derived stem cells (PNSCs). This was achieved by isolating PNSCs

from adult peripheral nerves and then expanding them in a suspension culture to prepare them for clinical applications [11, 12]. PNSCs exhibit an immunological profile similar to that of neural crest cells and have the capacity to differentiate into both mesenchymal lineages and neurons [11]. Notably, PNSC spheroids are capable of differentiating into Schwann cells and secreting high levels of neurotrophic factors, such as neurotrophin-3 (NT-3) and glial cell-derived neurotrophic factor (GDNF) [12]. Our research has demonstrated that a single intraspinal injection of PNSC spheroids into the site of injury can significantly improve therapeutic outcomes, leading to nerve regeneration and the restoration of neurological functions in a rat model of spinal cord injury, which shares pathophysiological mechanisms with TBI [13–17]. Furthermore, PNSC spheroids have been shown to promote neuronal regeneration and remyelination, reduce mechanical allodynia, and decrease inflammation by releasing a variety of neurotrophic and anti-inflammatory factors. However, we observed that the expression and secretion of NT-3 and GDNF by PNSC spheroids peaked at 3 days post-injection and then rapidly declined over the subsequent 3 weeks [11]. Based on these observations, we hypothesized that the neuroregenerative effects of PNSC spheroids could be augmented by repeated administrations, which would maintain high levels of neurotrophic factors for an extended period.

This study is a preclinical investigation designed to assess the impact of repeated intrathecal injections of PNSC spheroids on neuroregeneration in a rat model of TBI.

Materials and methods

Study design

PNSC spheroids were produced through a suspension culture technique, and their efficacy was subsequently evaluated. To investigate the advantages of multiple administrations of PNSC spheroids, rats were subjected to TBI induction. Behavioral assessments were performed at predetermined intervals to track recovery progress. At 6 weeks post-induction, the rats were euthanized to allow for extensive analyses, which included

histological examinations, magnetic resonance imaging (MRI) scans, and immunofluorescence staining to assess functional recovery (Fig. 1).

Tissue and reagents

Following the approval of the Institutional Review Board of Inje University College of Medicine (IRB No. 16–0147), surplus sciatic tissue from brain-deceased organ donors was acquired. *For this study, the donors' guardian provided written informed consent for participation in the study and the use of samples.* Porcine skin-derived collagen (MS Collagen®) and type I collagenase were obtained from MSBio (Seongnam, Korea) and Worthington Biochemical (Lakewood, NJ, USA), respectively. Growth factors, including recombinant epidermal growth factor (EGF), basic fibroblast growth factor (bFGF), β -nerve growth factor (NGF), and brain-derived neurotrophic factor (BDNF), were sourced from Peprotech (Rehovot, Israel), unless otherwise specified. All culture media, animal sera, and additional culture-related reagents were purchased from Gibco (Carlsbad, CA, USA).

Cell isolation and culture

PNSCs were isolated from donated peripheral nerves (PN) utilizing a previously described 3D organ culture method [11]. The epineurium and adjacent connective tissues were meticulously removed under a stereomicroscope. Subsequently, the PNs were finely chopped into 2- to 3-mm segments, rinsed with phosphate-buffered saline (PBS), and then dispersed in a chilled 0.25% neutral collagen mixture. This mixture, consisting of 100 mg of nerve fragments in 10 mL of neutral collagen solution, was transferred to a 100-mm tissue culture dish. It was then left to incubate in a moist chamber at 37 °C for 2 hours, facilitating the formation of a neutral collagen hydrogel that encapsulated the nerve fragments. This setup was further supplemented with 15 mL of organ culture medium containing 100 ng/mL EGF, 20 ng/mL bFGF, and 10 μ g/mL gentamicin mixed in Dulbecco's Modified Eagle Medium/Nutrient Mixture F-12 (DMEM/F12). After a 14-day cultivation period, the collagen hydrogels with embedded PN fragments and proliferating PNSCs were treated with 0.01% collagenase type I at 37 °C. This was done under dynamic conditions on an orbital shaker set to 25 rpm for 30 min to dissolve the hydrogel. The released PNSCs were then collected, centrifuged at $150 \times g$ for 10 min, and resuspended in cell culture medium (DMEM/F12 supplemented with 10 ng/mL EGF, 2 ng/mL bFGF, and 10% fetal bovine serum [FBS]). These PNSCs were then cultured in polystyrene dishes under standard monolayer conditions until they reached 80% confluence. At this point, they were harvested using trypsin-EDTA and replated at a density of 5,000 cells/cm². PNSCs at the sixth passage (P6) were

employed for analyzing transcriptional, immunophenotypic, and biological characteristics and for generating multicellular spheroids (PNSC spheroids) for subsequent transplantation studies, unless stated otherwise. For comparison, bone marrow-derived mesenchymal stem cells (BMSCs) were isolated via established methods [18] to serve as negative controls. Additionally, SH-SY5Y and RAW264.7 cell lines were obtained from ATCC (Manassas, VA, USA).

Suspension culture

After treatment with trypsin-EDTA, PNSCs were gathered and resuspended in a suspension-culture medium consisting of DMEM/F12 enriched with 2% human serum albumin. A total of 7.5×10^6 PNSCs were seeded in T75 Ultra-Low attachment cell culture flasks (Corning Inc., Corning, NY, USA). Following a 3-day incubation period, the formed PNSC spheroids were retrieved, rinsed thrice with PBS, mixed with a cryopreservation solution (NutriFreez D10, Sartorius), and subsequently cryopreserved for future use.

Immunophenotype

The immunophenotypic characteristics of PNSCs were evaluated using antibodies targeting markers associated with neural crest (NC)-lineage cells, Schwann cells, neuroglia, endothelial cells, and hematopoietic cells (Table S1). Marker expression levels were determined using flow cytometry (FACS Canto™ BD Biosciences, San Jose, CA, USA) or confocal microscopy (Zeiss LSM 510 Meta, Gottingen, Germany). For immunofluorescence analysis of spheroids, paraffin-embedded sections obtained 1, 2, and 3 days post-culture were incubated overnight at 4 °C with primary antibodies. Following this, sections were treated with isotype-specific secondary antibodies conjugated with Alexa Fluor and incubated at 37 °C for 30 min. Nuclei were stained using 2 μ g/mL diaminidino phenylindole (DAPI; Invitrogen, Waltham, MA, USA), and sections were mounted with ProLong® Gold antifade reagent (Invitrogen). For direct immunophenotyping, approximately 2×10^5 PNSCs were incubated with primary antibodies, followed by labeling with Alexa Fluor-conjugated anti-mouse, anti-rabbit, or anti-goat IgGs. The analysis was performed on a minimum of 10,000 events and 3,000 cells to ensure robust data.

mRNA expression

The transcriptional profiles of PNSCs were analyzed through reverse-transcription polymerase chain reaction (RT-PCR). Total RNA from BMSCs, PNSCs, and PNSC spheroids was extracted using TRIZOL-reagent® (Molecular Research Center Inc., Cincinnati, OH, USA), adhering to the provided protocol. The RNA concentration was measured with a NanoDrop® ND-1000

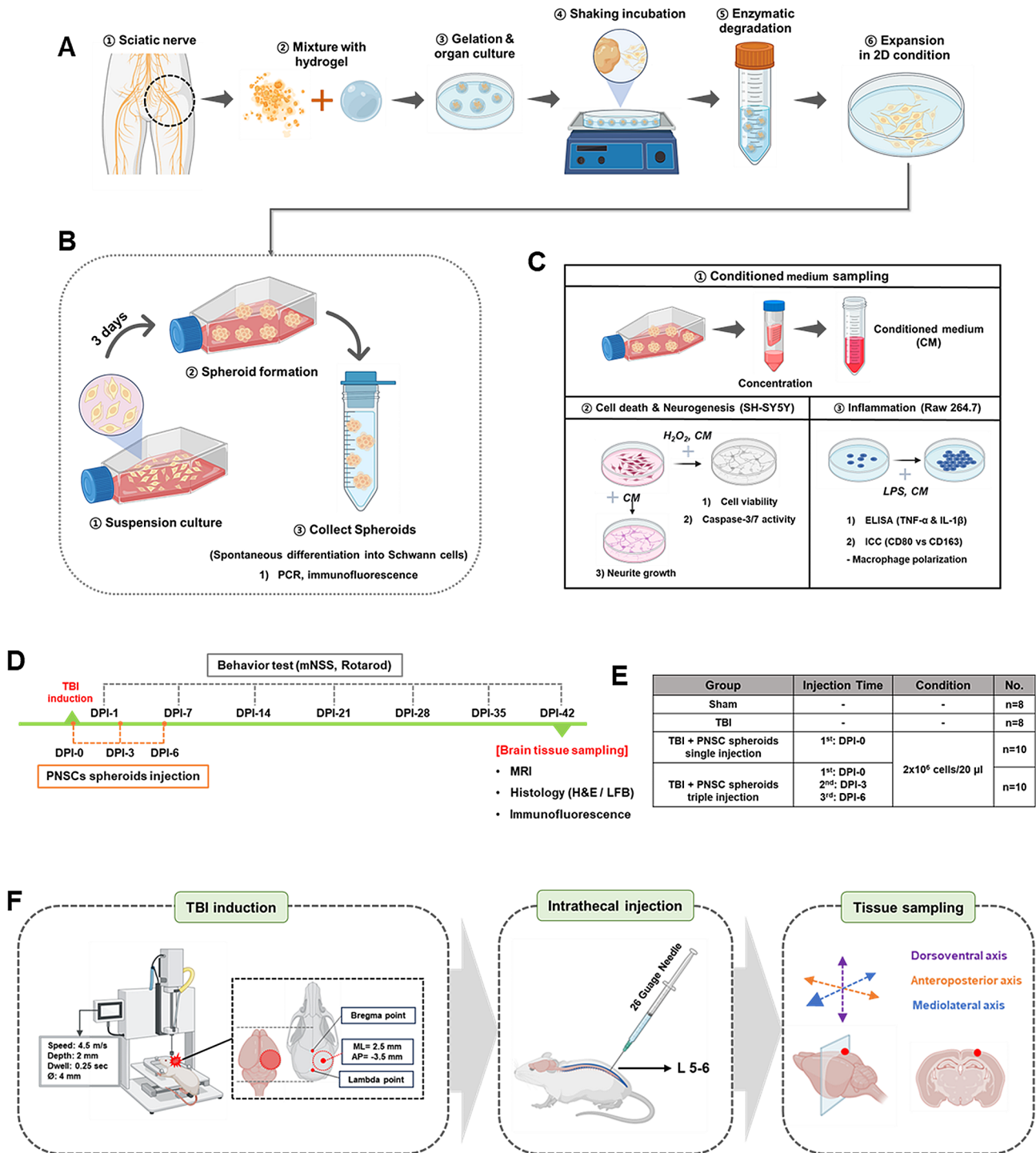


Fig. 1 Experimental Design Overview. **A:** Illustration of the peripheral nerve (PN) isolation process. **B:** Diagram detailing the preparation of peripheral nerve-derived stem cell (PNSC) spheroids via suspension culture. **C:** Overview of the methods employed to assess the therapeutic efficacy of prepared PNSC spheroids. **D:** Timeline and strategies for spheroid administration and subsequent evaluations post-traumatic brain injury (TBI). **E:** Categorization scheme utilized to examine the therapeutic impact of PNCS spheroids, based on injection frequency and the administered volume for each experimental group. **F:** Depiction of TBI model creation, including a schematic of the injection technique and the specific brain tissue sections selected for injury site analysis. [Figure created with BioRender.com]

spectrophotometer (Thermo Fisher Scientific, Wilmington, DE, USA). Subsequently, 1 µg of RNA was reverse-transcribed into first-strand cDNA using random primers and SuperScript® VILO™ (Invitrogen), in a GeneAmp 2400 PCR thermocycler (Applied Biosystems, Carlsbad, CA, USA). The cDNA synthesis conditions were set to 10 min at 25 °C, 50 min at 42 °C, and 15 min at 70 °C, before cooling to 4 °C. The expression of neurotrophic factors in BMSCs, PNSCs and PNSC spheroids was evaluated using a predesigned PCR array (Human Cytokine Primer Library I (HCA-1), Real Time Primers LLC, Elkins Park, PA). Quantitative real time PCR was carried out using SYBR Green Master Mix for qPCR (Applied Biosystems) and analyzed by an ABI Prism 7000 system (Applied Biosystems). The utilized program was as follows: an initial denaturation step for 2 min at 95 °C, and 40 cycles followed by 15 s at 95 °C and 1 min at 60 °C. The genes compared in this research are listed in Table S2. Gene expression for each sample was normalized to *beta actin*, a housekeeping gene, using the $2^{-\Delta\Delta C_t}$ method. The normalized values were then compared to those of BMSCs or PNSCs, processed similarly, to determine relative expression levels. All samples were analyzed in triplicate to ensure data reliability.

Neuroprotective effects and neurite outgrowth

Conditioned media (CMs) were produced from PNSCs and PNSC spheroids following a 3-day culture period in vehicle medium (DMEM/F12 supplemented with 0.1% calf serum) and subsequently concentrated using Amicon® Ultra-15 centrifugal filter units (Millipore, Billerica, MA, USA). The potential protective effects of these CMs were evaluated in an H₂O₂-induced cellular injury model. Initially, SH-SY5Y cells (5×10^4 cells) were plated in 48-well plates and cultured for 1 day, followed by treatment with 0.5 mM H₂O₂ either with or without the addition of CMs. After a 12-hour incubation period, the cells were rinsed with PBS and lysed using Cell-Lytic™ (Sigma Aldrich, St. Louis, MO, USA). Cell viability was assessed using a CyQuant GR dye (Invitrogen). The protective efficacy of CMs was further analyzed by measuring caspase-3/7 activity with fluorogenic substrates (Z-DEVD-aminoluciferin, Promega, Fitchburg, WI, USA). Additionally, the influence of CMs on neurite outgrowth and synaptic formation was investigated. SH-SY5Y cells were cultured on laminin-coated coverslips for 24 h. After fixation, the cells were immunostained with anti-neurofilament antibodies, and analyses of neurite length and synaptic formation were performed using ImageJ software. The analysis quantified the number of synapses per 100 µm of dendritic length to assess each determinant's contribution.

Anti-inflammatory effects

The anti-inflammatory properties of CMs derived from PNSCs and PNSC spheroids were evaluated through an assay utilizing RAW264.7 cells. The levels of tumor necrosis factor alpha (TNF-α) and interleukin-1β (IL-1β) secreted by lipopolysaccharide (LPS, Sigma Aldrich)-activated RAW264.7 cells were quantified using immunosorbent assay kit (R&D Systems, Minneapolis, MN, USA). Additionally, the influence of CMs on the polarization of macrophages from the pro-inflammatory M1 state to the anti-inflammatory M2 state was investigated. RAW264.7 cells, stimulated with lipopolysaccharide (LPS, Sigma Aldrich) and interferon-γ (Sigma Aldrich) in the presence or absence of CMs, were analyzed for the surface expression of M1 marker CD86 and M2 marker CD163. This expression was quantified using confocal microscopy to assess the CMs' potential to modulate macrophage polarization.

Preparation of PNSC spheroids

Prior to their administration to the animals, the cryopreserved vials of PNSC spheroids were rapidly thawed. The spheroids were then collected in alpha-Modified Eagle Medium (α-MEM, Gibco) supplemented with 1% FBS (Gibco) and centrifuged at 1,000 rpm for 3 min. The supernatant was carefully removed, and the concentration of the spheroids was adjusted to a density of 2.0×10^6 cells/µl for injection.

Animals and TBI modeling procedures

Animal experiments were conducted after receiving approval from the Institutional Animal Care and Use Committee of the CHA University School of Medicine (IACUC-220189). The animal studies were conducted following ARRIVE guidelines (Animal Research: Reporting of In vivo Experiments). Nine-week-old female adult Sprague-Dawley rats (220–250 g) were purchased from Koatech (Pyeongtaek, Korea). We chose female rats because they typically show higher levels of natural antioxidant enzymes compared to males [19, 20], which could enhance recovery outcomes. Additionally, we avoided using male rats due to concerns about aggression when housed together [21]. To minimize stress from environmental changes, the animals underwent a 1-week acclimatization period before being subjected to procedures at the age of 10 weeks. They were maintained in a facility with a 12-hour light/dark cycle, temperature controlled between 22 °C and 25 °C, and humidity maintained at 40–60%, with *ad libitum* access to food and water.

Prior to the surgical procedure, the rats were anesthetized using a combination of zolazepam and tiletamine (Zoletil, 50 mg/kg, intraperitoneally, Virbac Laboratories, Virbac, France) and xylazine (Rompun, 10 mg/kg, intraperitoneally, Bayer, Seoul, Korea). Preoperative

preparation involved shaving the head and disinfecting the surgical area with povidone-iodine and 70% ethanol. A controlled cortical impact (CCI) model for simulating TBI was established using a Precision Impactor Device 68,900II (RWD Life Science, Shenzhen, China). The procedure started with an incision to expose the skull, followed by a 5-mm-diameter craniotomy over the right parietal region, located 3.5 mm posterior to the coronal suture and 2.5 mm lateral to the sagittal suture, performed with a hand drill. The impact was delivered using an impactor tip with a diameter of 4 mm, on the exposed dura mater at a velocity of 4.5 m/s, to a depth of 2.0 mm, with a dwell time of 250 ms [22]. Post-injury, the incision was sutured after achieving hemostasis with sterile gauze and cotton swabs, followed by additional disinfection with povidone-iodine. The animals were then treated with ketoprofen for pain relief, cefazolin as an antibiotic, and saline for hydration. Postoperative care included maintaining the animals on a heating pad set to 39 °C until they fully recovered. Cyclosporine (Cipol-N, Chong Kun Dang Pharmaceutical Corp., 100 mg/L) was administered orally to all animals starting 2 days before the surgery and continuing until 6 weeks post-surgery, at which point the animals were euthanized [23].

Experimental groups and intrathecal injections of spheroids

In this study, 36 experimental animals were allocated into four groups: (1) sham ($n=8$); (2) TBI ($n=8$); (3) TBI plus single injection of PNSC spheroids ($n=10$, henceforth referred to as the “single injection.” group); and (4) TBI plus triple injections of PNSC spheroids ($n=10$, henceforth referred to as the “triple injection.” group) (Fig. 1E).

For the interventions, PNSC spheroids (a total of 2×10^6 cells, approximately 11217.05 spheroids/20 μ L per injection) were administered into the intrathecal space. The single inj. group received a one-time injection immediately following the induction of the CCI model (day 0), whereas the triple inj. group was given three injections at 3-day intervals (i.e., on days 0, 3, and 6). Prior to the intrathecal injection, the spheroids were prepared in a Hamilton syringe equipped with a 26G needle. The lumbar region of each anesthetized rat was prepared by shaving and disinfecting with povidone-iodine and 70% ethanol-soaked gauze. The procedure involved locating the space between the fifth and sixth lumbar vertebrae by identifying the most convex bone in the lumbar region and following the pelvic bones towards the spine. The needle was then carefully inserted obliquely into this space, ensuring correct placement by observing a “tail flick” response from the rat. The PNSC spheroids were injected by intrathecal administration at a rate of 10 μ L per minute. Upon successful injection, the needle was maintained in place for 1 min to ensure proper delivery,

then gently withdrawn, and the site was again disinfected with povidone-iodine.

Behavioral assessments

Modified neurological severity score (mNSS)

Neurological function was evaluated using the Modified Neurological Severity Score (mNSS) to assess both sensory and motor capabilities. This scoring system ranges from 0 to 18, where 0 represents normal functionality and 18 signifies maximum impairment. Scores from 1 to 6 are categorized as mild injury, 7 to 12 as moderate injury, and 13 to 18 as severe injury [24]. The mNSS test was performed on days 1, 7, 14, 21, 28, 35, and 42 following CCI induction. The assessment was carried out by two researchers who were blinded to the group allocations, ensuring an unbiased evaluation of the differences among groups.

Rotarod test

The rotarod test was utilized to assess advanced motor skills, including the ability to bear weight and coordinate movements of the hind limbs. For this test, each animal was placed on a rotating cylinder (rotarod), and the duration it could stay atop the cylinder was recorded. The speed of the rotarod was gradually increased from 4 rpm to 40 rpm over a 5-minute period. The test concluded either when the animal fell from the cylinder or managed two consecutive rotations without attempting to walk on the rotating surface, merely clinging to the apparatus. To ensure reliable performance, all animals underwent training for 3 days before the CCI procedure, and rotarod performance was recorded three times the day before surgery to establish an average baseline duration (in seconds). The reported values for the rotarod test are the mean durations across these three trials, which helps to provide unbiased data [25]. Furthermore, the rotarod cylinder was sanitized with 70% ethanol between each trial to eliminate odors and disinfect the equipment.

Magnetic resonance imaging (MRI)

To assess the extent of brain injury, brain tissues were harvested 6 weeks after CCI induction and analyzed using T2-weighted MRI with a 9.4 T system (Bruker BioSpec, Billerica, MA, USA). To collect brain tissue, rats were first anesthetized and then euthanized by transcardiac perfusion with saline followed by 4% paraformaldehyde (PFA). After perfusion and fixation in 4% PFA, ex vivo MRI scanning was conducted. T2-weighted images were obtained in the coronal plane using the following parameters: repetition time=2.5 s, field of view=25×25 mm, slice thickness=1 mm, matrix size=128×128, and echo time=76 ms. Each tissue sample scan lasted approximately 10 min. The volume of brain injury was determined by calculating the sum of

the lesion areas (in mm²) across three MRI slices (focusing on the slice depicting the largest lesion) and multiplying by the thickness of a slice (1 mm). This analysis was performed using ImageJ software (National Institutes of Health, Bethesda, MD, USA) [26].

Histological analysis

After perfusion and fixation in 4% PFA, rats were processed into paraffin blocks, and 3- μ m-thick sections of the damaged brain tissue were prepared using a rotary microtome. Before histological staining, the slides underwent deparaffinization in xylene and were rehydrated through a graded series of ethanol solutions at concentrations of 99.9%, 95%, 90%, 80%, and 70%.

Hematoxylin and eosin (H&E) staining

H&E staining was conducted to evaluate differences in brain tissue loss. Sections were stained with Harris hematoxylin solution, followed by decolorization with 1% alcohol hydrochloric acid and neutralization in 1% ammonia water. The tissues were then stained with eosin to highlight the cytoplasm, dehydrated through a series of ethanol concentrations (70%, 80%, 90%, 95%, and 99.9%), and cleared in xylene. Finally, coverslips were applied using a lipid-soluble mounting medium (Canada balsam). Digital images of all H&E-stained tissue slides were captured using a digital slide scanner (Zeiss Axio Scan.Z1, Carl Zeiss, Oberkochen, Germany). The areas of the damaged ipsilateral hemisphere (right) and the unaffected contralateral hemisphere (left) were delineated and quantified as a percentage of total area using ImageJ software (National Institutes of Health) [27]. Additionally, live and necrotic neurons in the hippocampal regions CA1 and CA3 were identified and quantified [28].

Luxol fast blue (LFB) staining

LFB staining was performed to assess the extent of remyelination in brain tissue. Following the manufacturer's instructions provided with the LFB staining kit (Abcam, Cambridge, United Kingdom; #ab150675), tissue sections were immersed in LFB staining solution for 24 h at room temperature. Differentiation was achieved with a 0.05% lithium carbonate solution and 70% ethanol for 5 s, until the gray matter appeared colorless while the white matter retained a blue hue. The neuronal cytoplasm was subsequently stained with cresyl echt violet. Following staining, the sections were dehydrated through a graded ethanol series (70%, 80%, 90%, 95%, and 99.9%) and clarified in xylene. Coverslips were applied using a lipid-soluble mounting medium (Canada balsam). Digital images of the LFB-stained sections were captured using a digital slide scanner (Zeiss Axio Scan.Z1, Carl Zeiss) for analysis. For quantitative assessment, three equally sized regions of interest were selected across the corpus

callosum in both the ipsilateral and contralateral hemispheres to evaluate thickness. Analysis was performed using ImageJ software (National Institutes of Health), and results were expressed as a percentage change relative to the contralateral side, with 100% indicating no difference from the contralateral hemisphere [29].

Immunofluorescence staining

For immunofluorescence analysis, brain tissue sections were rehydrated and underwent antigen retrieval by boiling for 10 min at 95 °C, followed by a 30-minute cooling period in either citrate buffer at a pH of 6.0 (Sigma Aldrich, #C9999-1 L) or Tris-EDTA at a pH of 9.0 (Biosesang, Yongin, Korea; #TR2220-050-90), depending on the specific requirements of each antibody. After antigen retrieval, sections were blocked with a 5% bovine serum albumin (BSA) solution for 1 h at room temperature to prevent nonspecific binding. Primary antibodies were then applied at the recommended dilution in 5% BSA and incubated on the sections for 2 h at room temperature. The sections were then washed three times with 1% Tween 20 in 1 \times PBS to remove excess primary antibody, followed by incubation with the secondary antibody diluted 1:200 in the diluent for 1 h at room temperature. Nuclear staining was performed by applying DAPI (Thermo Fisher, #D1306) diluted 1:10,000 in Dulbecco's PBS (DPBS, Cytiva, #SH30028.02) for 10 min after the secondary antibody washing steps. The sections were then washed with PBS-T before mounting the coverslips using a water-soluble fluorescent mounting medium (Dako Fluorescent Mounting Medium, Agilent, Santa Clara, CA, USA, #S3023). Detailed specifications of the primary and secondary antibodies, including the dilution ratios, are listed in Table S1. Digitally scanned images of all stained sections were captured using a digital slide scanner (Zeiss Axio Scan.Z1, Carl Zeiss, Oberkochen, Germany). The qualitative assessment of immunofluorescence involved analyzing images of the lesion site using ImageJ software (National Institutes of Health). This analysis quantified the percentage of the area positive for staining relative to the total area (%) and counted the number of cells with positively stained nuclei or cytoplasm [30, 31]. For the Sholl analysis of microglia, a total of 30 random IBA-1 positive microglia per group were morphologically evaluated. The images were converted from color to binary, and the threshold was manually adjusted until only the cell body and branches of the microglia were visible. The number of microglial branches intersecting each circle was counted, and a Sholl plot was created for each cell. These individual plots were then averaged to obtain an average Sholl plot for each animal [32].

Statistical analysis

Data obtained from MRI and histological evaluations were processed and analyzed using ImageJ software (National Institutes of Health). The results are presented as the mean \pm standard error of the mean. Statistical analysis was performed using one-way ANOVA, with post hoc comparisons made via the Tukey test to identify differences among the groups. Graphical representations of the data and statistical analyses were generated using GraphPad Prism (version 8.0.2, GraphPad Software, La Jolla, CA, USA). A p -value of less than 0.05 was considered to indicate statistical significance. Detailed explanations of the statistical significance and analyses are included in the captions accompanying each figure.

Results

PNSCs exhibit characteristics typical of uncommitted neural crest-lineage cells

A hydrogel-supported organ culture system enabled the proliferation and migration of PNSCs from the PN into the surrounding hydrogel matrix. Notably, PNSC outgrowth into the hydrogel was initially detected within 1 day of culture, and the extent of outgrowth increased in a time-dependent manner (Fig. 2A). By day 14 of culture, cells that had migrated out of the hydrogels were isolated and subsequently cultured in a monolayer format (Fig. 2B). Flow cytometry further confirmed the identity of PNSCs as uncommitted NC-lineage cells, as demonstrated by the consistent expression of markers such as Nestin, p75, Sox10, and AP2 α (Fig. 2C). Conversely, PNSCs lacked expression of glial markers such as GAP43, GFAP, S100 β , and MPZ (Fig. S1), reinforcing their classification as uncommitted neural crest lineage cells.

PNSC spheroids exhibit Schwann cell-like reparative properties

In vitro experiments assessed the potential of PNSCs to differentiate into peripheral glial cells. Without the addition of differentiation-inducing factors, PNSCs were cultured on ultra-low attachment plates to promote homotypic cell-to-cell interactions. Within 3 days, PNSCs spontaneously formed multicellular spheroids (Fig. 2D) and began expressing proteins associated with peripheral glia, including GFAP, GAP43, MPZ, and S100 β (Fig. 2E). This observation suggests that PNSC spheroids can naturally differentiate into Schwann cells through spheroid formation, without the need for external chemical or growth factor stimuli.

Furthermore, PNSCs showed higher expression of neurotrophic factor mRNAs than BMSCs (Fig. 2F). Upon transitioning into multicellular spheroids, PNSC spheroids significantly increased the expression of neurotrophic factor mRNAs, such as ephrin, NGF, GDNF, BDNF, and neurotrophin (NTF), compared to both

PNSCs and BMSCs (Fig. 2G-I). An analysis of PNSCs and PNSC spheroids relative to BMSCs revealed an over 2-fold increase in expression with statistical significance (p -values) for several factors (Fig. 2I). Notably, NTF3, ephrin B3, LIF, GDNF, and ZFP91 showed significantly higher expression levels in both PNSCs and PNSC spheroids. In contrast, the expression levels of neuregulin 2/3, ephrin 2/3, and ephrin B1 were elevated specifically in PNSC spheroids.

Conditioned medium derived from PNSC spheroids exhibits neuroprotective and anti-inflammatory effects

Our analysis of the neuroprotective and neurotrophic properties of PNSCs and their spheroids revealed that exposure to oxidative stress (H₂O₂) in SY-SH5Y cells led to higher levels of cell death and caspase activity. However, treatment with CM from either PNSCs or PNSC spheroids in the presence of H₂O₂ increased cell viability (to 109.0 \pm 1.4% and 114.7 \pm 7.4% with 100% CM, respectively) and reduced caspase activity (to 1.66 \pm 0.16 and 1.54 \pm 0.09-fold with 100% CM, respectively) in a concentration-dependent manner (Fig. 3A). Although the CM from PNSC spheroids showed slightly higher neuroprotective activities than the CM from PNSCs alone, the difference was not statistically significant.

Further experiments demonstrated the ability of these CMs to stimulate neurite outgrowth and synapse formation in vitro. The presence of CM from PNSCs (66.1 \pm 2.5 μ m with 100% CM) and PNSC spheroids (75.1 \pm 2.4 μ m with 100% CM) significantly increased the average neurite length compared to vehicle media (45.0 \pm 2.5 μ m) in a concentration-dependent manner (p < 0.05, Fig. 3B, C). Neurite branching also significantly increased in cells treated with CM from PNSCs (4.7 \pm 0.3 with 100% CM) and PNSC spheroids (5.7 \pm 0.3 μ m with 100% CM) compared to vehicle medium (2.5 \pm 0.2 μ m; p < 0.05, Fig. 3B, C). These findings highlight the significant role of PNSCs and PNSC spheroid-derived secretomes in neuronal repair and regeneration.

Inflammatory responses can hinder the repair processes following brain injury, prompting efforts to mitigate such responses [33]. The secretion of TNF- α and IL-1 β , which are key pro-inflammatory mediators [34], was reduced when RAW264.7 cells, stimulated by LPS, were treated with CM from PNSCs and PNSC spheroids (to 532.0 \pm 152.8 and 64.7 \pm 11.1 pg for TNF- α , and to 232.3 \pm 49.7 and 85.3 \pm 9.3 pg for IL-1 β with 50% CM, respectively) compared to vehicle medium (1759.3 \pm 166.2 and 537.7 \pm 120.3 pg, respectively; p < 0.05, Fig. 3D). This indicates a potent anti-inflammatory action of the CMs.

Upon injury, regenerative inflammation induces tissue regeneration, which results from in-situ macrophage polarization involving a transition from pro-inflammatory (M1) to anti-inflammatory (M2) phenotype [35].

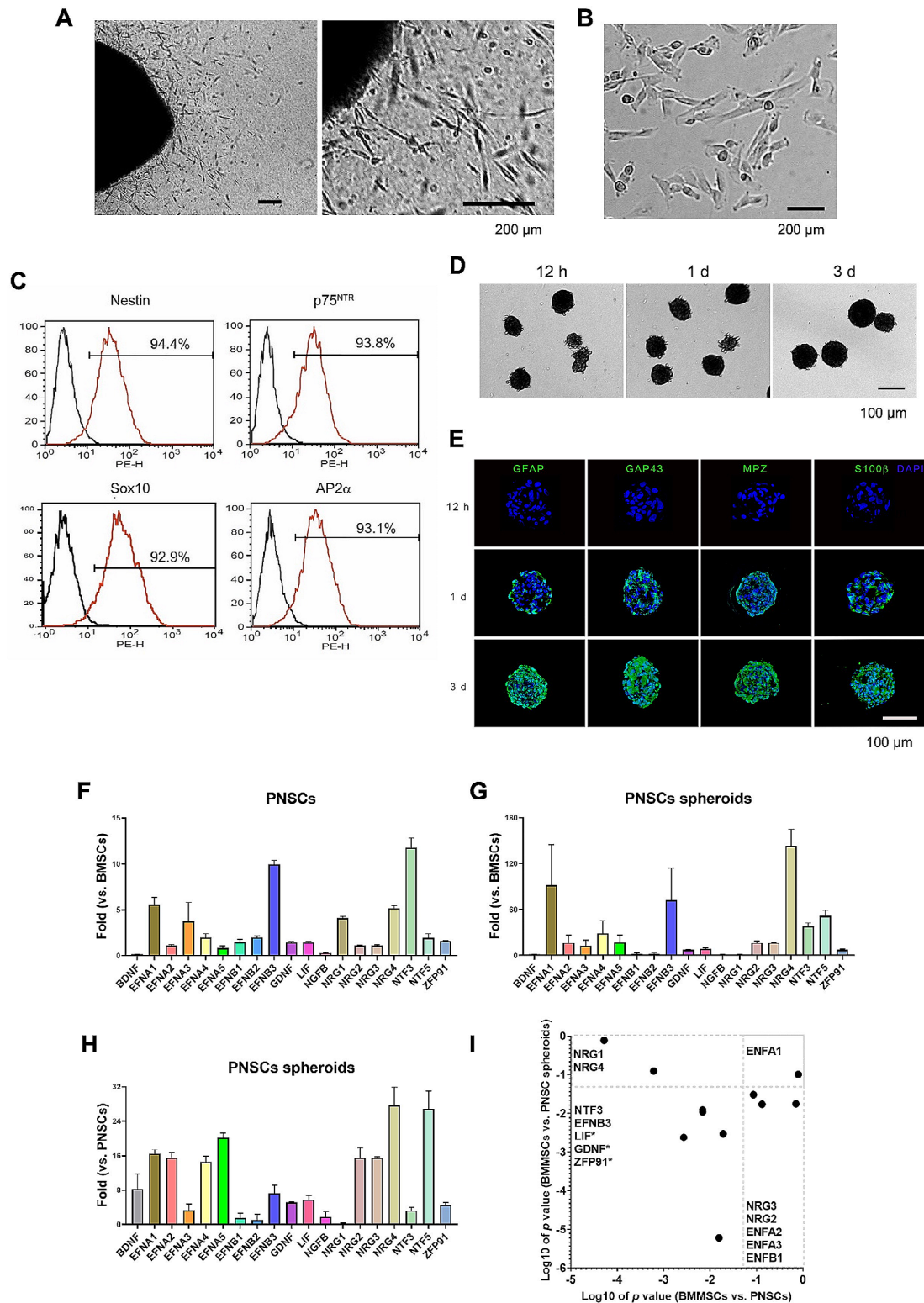


Fig. 2 Characterization of peripheral nerve-derived stem cells (PNSCs) and their Schwann-like properties in spheroids. **A:** Hydrogel-supported 3D organ culture from peripheral nerve showing cell migration and outgrowth, presented in both low and high magnification views. **B:** Bipolar spindle-shaped morphology of outgrown cells under monolayer culture conditions. **C:** Flow cytometry analysis demonstrating PNSCs' expression of neural crest-lineage markers such as Nestin, p75, Sox10, and AP2 α . **D:** Formation of multicellular PNSC spheroids via suspension culture over time. **E:** Expression of peripheral glia-related proteins (GAP43, GFAP, MPZ, and S100 β) by PNSC spheroids. **F - I:** Increased expression of neurotrophic mRNAs (ephrin, NGF, GDNF, BDNF, and NT) in PNSC spheroids compared to PNSCs and bone marrow-derived stem cells (BMSCs)

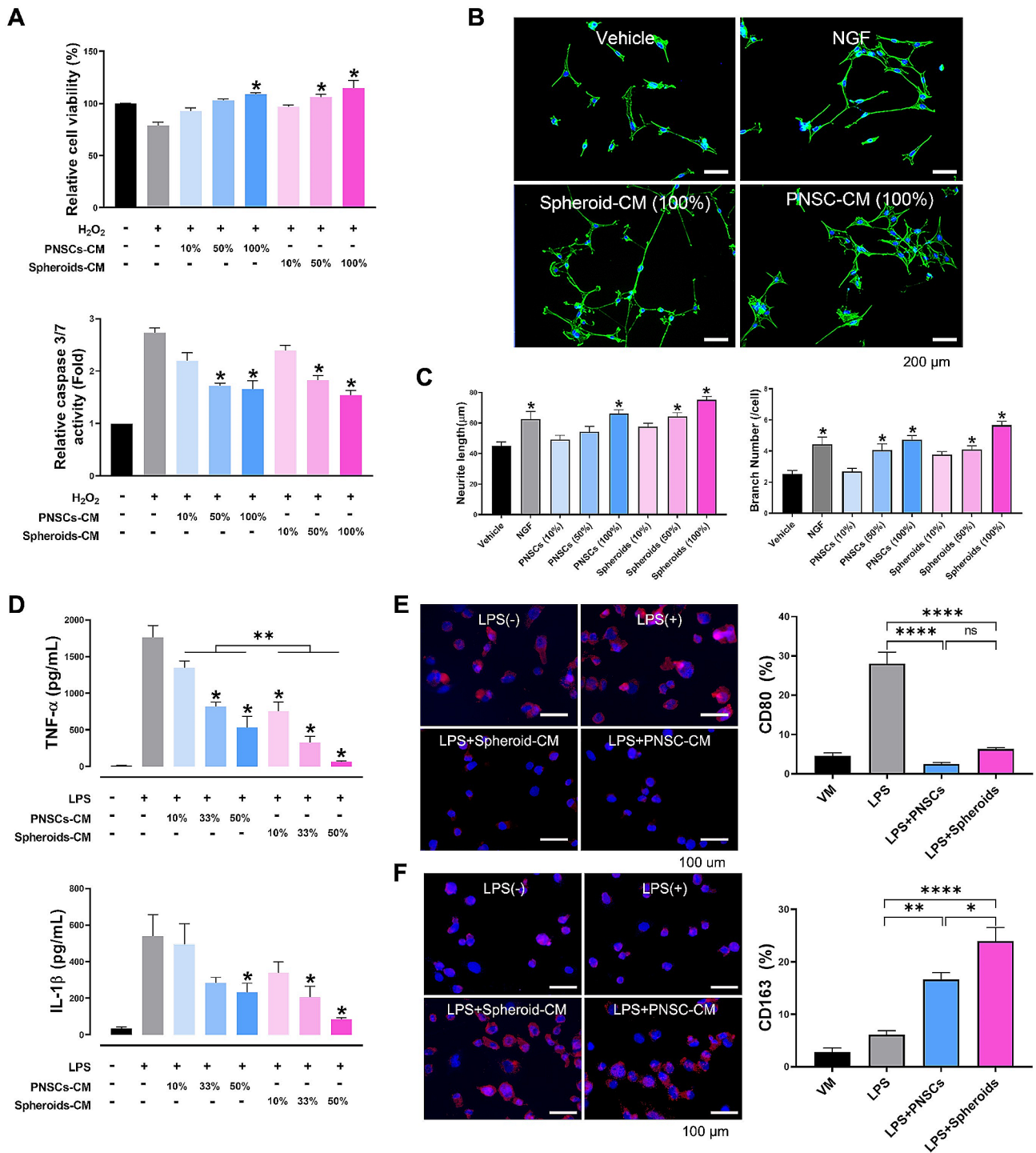


Fig. 3 Neuroprotective and neurogenic effects of peripheral nerve-derived stem cell (PNS) spheroids. **A:** Treatment with conditioned media (CMs) from PNSCs or PNSC spheroids increased cell viability and decreased caspase activity in a concentration-dependent manner, with no significant difference observed between treatments from PNSCs and their spheroids. **p* < 0.05 compared to the H₂O₂-treated group. **B, C:** SH-SY5Y cells exhibited significant increases in neurite outgrowth, both in length and number, following treatment with CMs from PNSCs and PNSC spheroids. **p* < 0.05 compared to vehicle medium. ***p* < 0.01 compared to PNSC. **D:** TNFα and IL-1β levels significantly reduced after treatment with CMs from PNSCs and PNSC spheroids, in a concentration-dependent manner. **p* < 0.05 compared to vehicle medium. ***p* < 0.01 compared to PNSC. **E, F:** LPS stimulation elevated CD80+M1 and CD163+M2 macrophage populations; CMs from PNSCs significantly reduced the M1 population. Importantly, the CM from PNSC spheroids induced a significantly greater M2 polarization compared to the CM from PNSCs. **p* < 0.05 compared to lipopolysaccharide-stimulated cells. ***p* < 0.01 compared to PNSC-treated cells

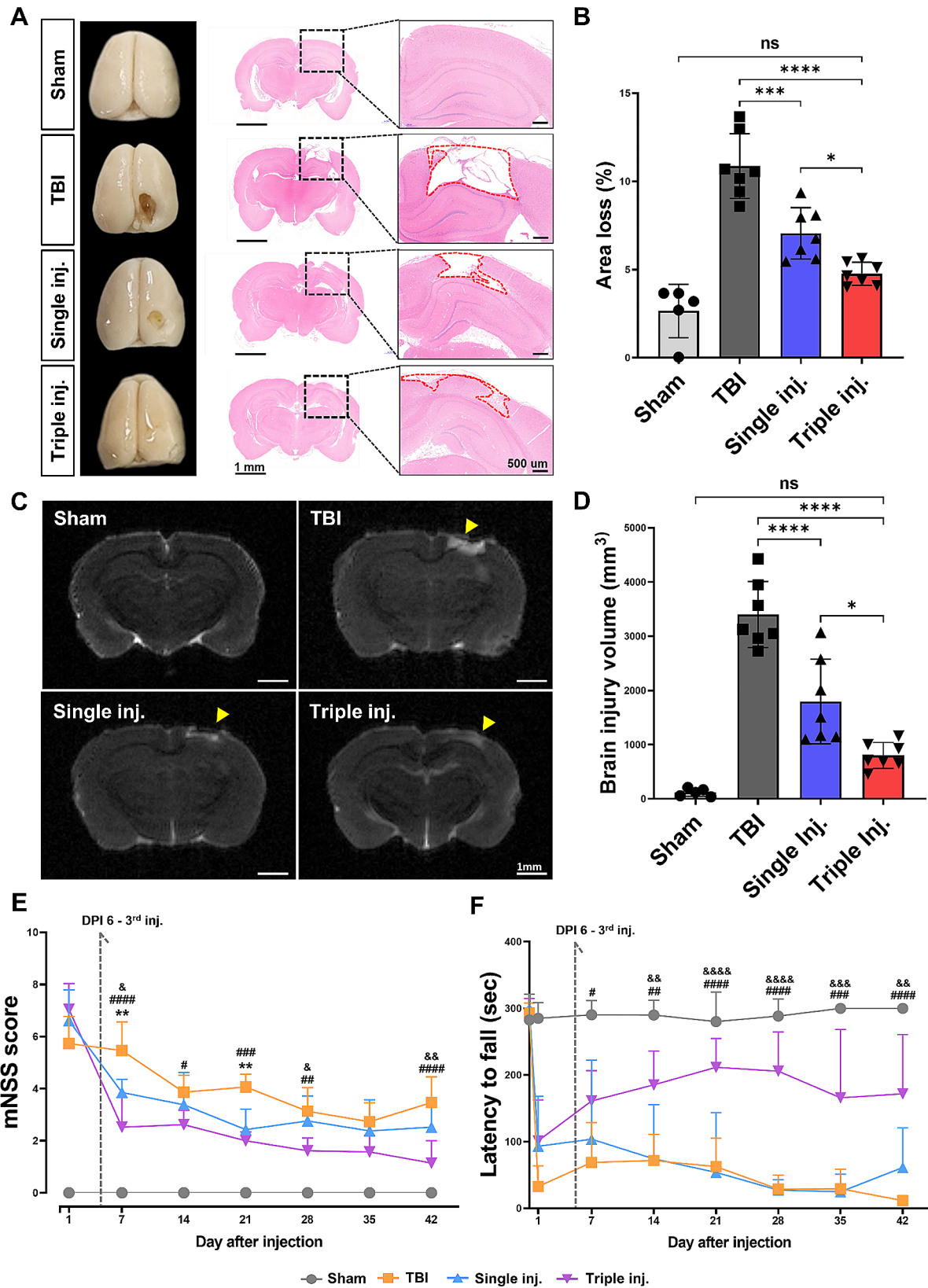


Fig. 4 (See legend on next page.)

(See figure on previous page.)

Fig. 4 Enhanced structural and functional recovery following repeated intrathecal injections of peripheral nerve-derived stem cell (PNSC) spheroids. **A, B:** Representative images of brain tissue with hematoxylin and eosin (H&E) staining (**A**) and a quantitative analysis of the area of loss (**B**) 6 weeks post-traumatic brain injury (TBI) across four experimental groups. **C, D:** T2-weighted MRI images at 6 weeks post-TBI (**C**) along with a corresponding quantitative analysis of brain injury volume (**D**). Statistical significance for **B** and **D** was assessed using one-way ANOVA followed by the Tukey correction. * $p < 0.05$; ** $p < 0.01$; *** $p < 0.001$; **** $p < 0.0001$; ns, not significant. **E, F:** The mNSS test (**E**) and rotarod test (**F**) performed to assess advanced motor, sensory, and general motor function post-TBI on days 1, 7, 14, 21, 28, 35 and 42. Statistical significance for E and F was determined using two-way ANOVA with the Tukey correction. ** $p < 0.01$, TBI group vs. single inj. group; $p < 0.05$, ## $p < 0.01$, ### $p < 0.001$, #### $p < 0.0001$, TBI group vs. triple inj. group; & $p < 0.05$, && $p < 0.01$, &&& $p < 0.001$, &&&& $p < 0.0001$, single inj. group vs. triple inj. group. All data are expressed as mean \pm standard deviation (SD)

An examination of the role of these CMs in macrophage polarization from a pro-inflammatory M1 phenotype to a reparative M2 phenotype revealed significant shifts. LPS-induced M1 macrophage populations ($28.0 \pm 5.8\%$) were substantially reduced by CM treatment from PNSCs and PNSC spheroids (to $2.5 \pm 0.8\%$ and $6.4 \pm 0.6\%$, respectively; $p < 0.001$, Fig. 3E), while M2 populations were increased (to $16.6 \pm 2.6\%$ and $24.0 \pm 5.2\%$, respectively; $p < 0.05$ and $p < 0.001$, respectively, Fig. 3F). The CM from PNSC spheroids showing a notably stronger M2 polarization effect than the CM from PNSCs alone ($p < 0.05$). In summary, CM derived from PNSCs and PNSC spheroids demonstrates a capacity to reduce pro-inflammatory cytokine secretion and promote anti-inflammatory M2 macrophage polarization, showcasing their potential as anti-inflammatory agents.

Triple intrathecal injections of PNSC spheroids improve structural and functional recovery following TBI

To evaluate the therapeutic potential of PNSC spheroids, we administered them intrathecally in a CCI rat model, comparing the effects of single (single inj.) and triple injections (triple inj.). Six weeks post-TBI, H&E staining of brain sections was performed to assess tissue damage. The extent of tissue loss was significantly less in the triple inj. group than in both the TBI and single inj. groups (Fig. 4A). H&E staining revealed the greatest area of loss in the TBI group (Fig. 4A, B). The triple inj. group exhibited a substantial reduction in the area of loss ($4.761 \pm 0.6511\%$) compared to the TBI group ($10.87 \pm 1.835\%$; $p < 0.0001$) and the single inj. group ($7.055 \pm 1.459\%$; $p < 0.05$) (Fig. 4A, B). T2-weighted MRI analysis further demonstrated that the triple inj. group ($800.2 \pm 239.5 \text{ mm}^3$) experienced significantly less brain edema than the TBI group ($3401 \pm 609.5 \text{ mm}^3$; $p < 0.0001$) and the single inj. group ($1797 \pm 781.3 \text{ mm}^3$; $p < 0.05$) (Fig. 4C, D), suggesting that injections of PNSC spheroids not only protected neurons, but also mitigated edema following TBI, with triple injections proving more beneficial than a single dose.

We also examined the impact of triple PNSC spheroid injections on the recovery of sensory and motor functions. Initially, all injured rats displayed elevated mNSS scores on the first day post-TBI (Fig. 4E). Over time, both the single and triple inj. group showed a decrease in mNSS scores compared to the TBI group, with the triple

inj. group demonstrating significantly improved neurological function by the sixth week post-TBI compared to the single inj. group (Fig. 4E). Furthermore, advanced motor skills, such as hindlimb coordination and weight-bearing ability assessed by the rotarod test, improved markedly in the triple inj. group relative to both the TBI and single inj. groups (Fig. 4F). These findings suggest that triple injections of PNSC spheroids effectively enhance sensory and motor recovery, indicating that this treatment may protect the cerebral cortex areas essential for sensorimotor functions from tissue loss, thereby facilitating functional recovery.

Triple intrathecal injections of PNSC spheroids promote remyelination following TBI

To assess the remyelination of the brain post-TBI, we utilized LFB staining and myelin basic protein (MBP) immunofluorescence staining. These techniques specifically target myelin to detect remyelination. The corpus callosum, a significant myelinated fiber bundle facilitating communication between the brain's hemispheres, served as a focal point for the remyelination assessment [36]. Therefore, the thickness of the corpus callosum was examined by LFB to determine remyelination (Fig. 5A). In the triple inj. group, the thickness of the corpus callosum indicated marked remyelination ($77.25 \pm 10.84\%$), showing a significant improvement over the TBI group ($45.07 \pm 12.47\%$; $p < 0.001$) and the single inj. group ($58.06 \pm 13.31\%$; $p < 0.05$) (Fig. 5A, B). However, no significant difference was observed between the TBI and single inj. groups (Fig. 5A, B).

MBP immunostaining further corroborated remyelination at and around the injury site, including within the corpus callosum (Fig. 5C). The analysis revealed higher levels of myelin formation in both the single group ($24.40 \pm 1.693\%$; $p < 0.0001$) and triple inj. group ($29.87 \pm 2.178\%$; $p < 0.0001$) than in the TBI group ($16.42 \pm 2.821\%$). Notably, myelin regeneration was significantly more pronounced in the triple inj. group ($29.87 \pm 2.178\%$) than in the single inj. group ($24.40 \pm 1.693\%$; $p < 0.01$) (Fig. 5C, D). These findings confirm that the strategy of administering triple injections of PNSC spheroids is highly effective in promoting myelin formation post-TBI. The observed increase in corpus callosum thickness and MBP expression in the triple

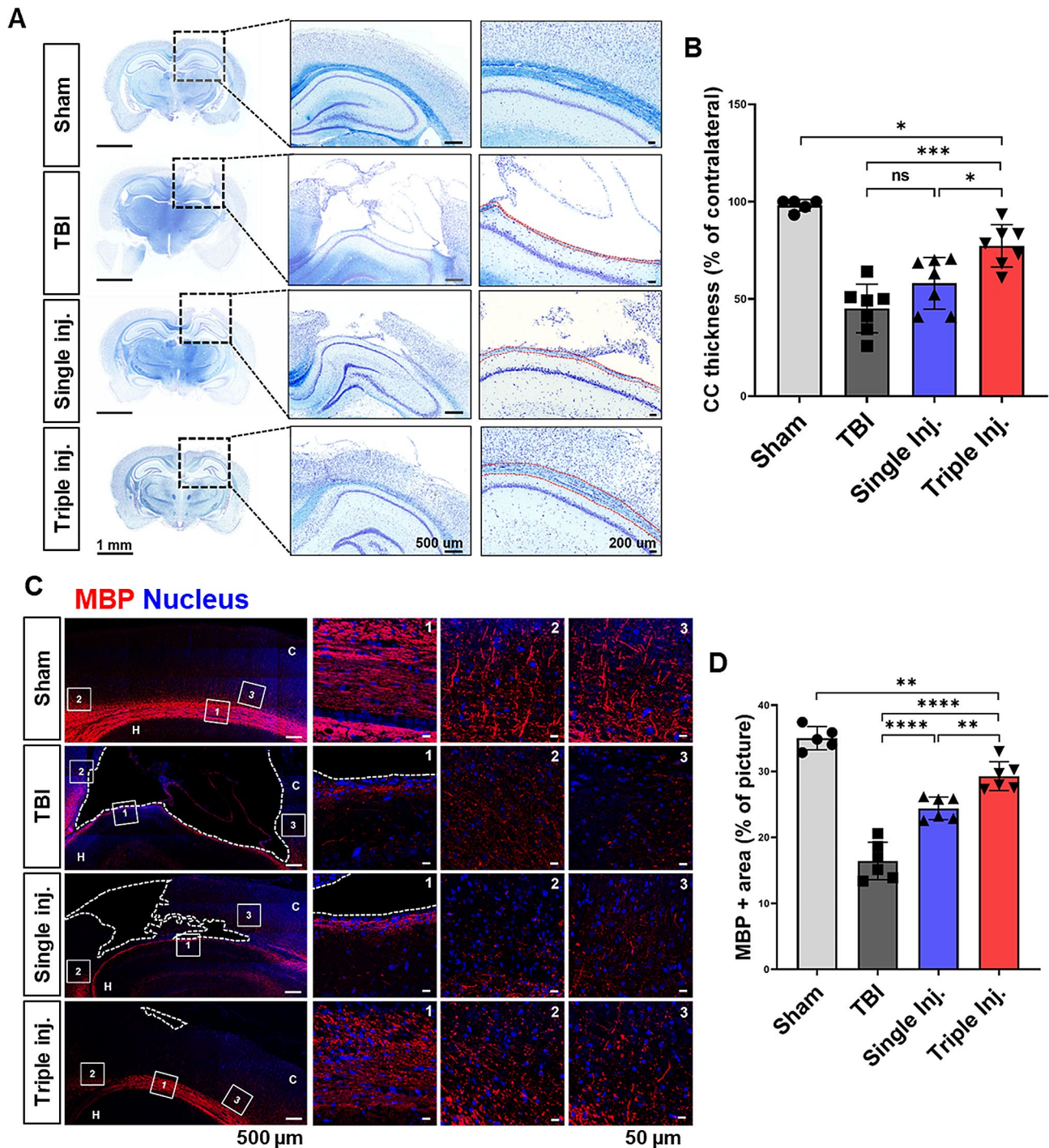


Fig. 5 Enhanced remyelination following repetitive intrathecal injections of PNSC Spheroids. **A, B:** Show representative images of Luxol fast blue (LFB) staining (**A**) to visualize myelination and a quantitative analysis of corpus callosum thickness (**B**) in coronal brain sections from each group, 6 weeks post-traumatic brain injury. **C, D:** Display immunofluorescence staining for myelin basic protein (MBP) (**C**) to identify myelin, alongside a quantitative analysis of the MBP-positive area (**D**). In the images, MBP is marked in red and nuclei are stained blue. The labels C and H denote the cortex and hippocampus, respectively. Statistical significance for **B** and **D** was assessed using one-way ANOVA followed by the Tukey correction. * $p < 0.05$; ** $p < 0.01$; *** $p < 0.001$; **** $p < 0.0001$; ns, not significant. All data are expressed as mean \pm standard deviation (SD)

injection group underscores the substantial impact of induced remyelination on white matter repair.

Triple intrathecal injections of PNSC spheroids mitigate neuronal loss and promote axonal regeneration post-TBI

To evaluate neuronal regeneration and cytoskeletal recovery, immunofluorescence staining was performed using NeuN, a neuronal marker, and neurofilament, indicative of the mature neuronal cytoskeleton (Fig. 6A).

In the cortical region adjacent to the injury site, the greatest restoration of the cytoskeleton was observed in the triple inj. group ($17.70 \pm 3.824\%$), significantly surpassing both the TBI ($5.831 \pm 0.345\%$; $p < 0.0001$) and single inj. groups ($11.20 \pm 1.414\%$; $p < 0.001$) (Fig. 6B, C). The CA1 area of the hippocampus, which is crucial for memory processes [37], also exhibited superior recovery in the PNSC spheroid-injected groups compared to the TBI group ($4.822 \pm 0.874\%$; $p < 0.0001$). Specifically, the

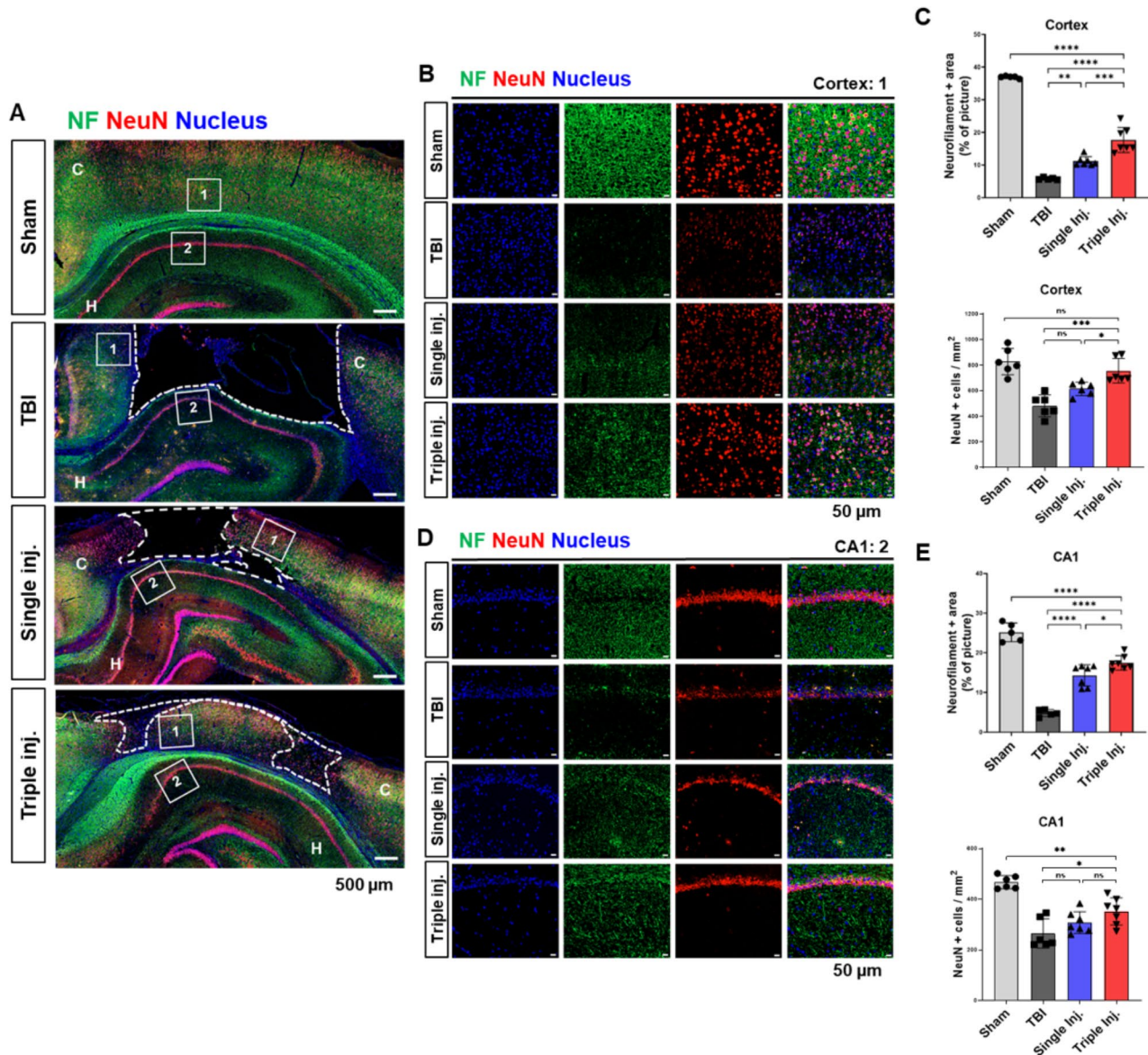


Fig. 6 Mitigation of neuronal loss and promotion of axonal regeneration following triple injections of peripheral nerve-derived stem cell (PNSC) spheroids post-traumatic brain injury (TBI). **A**: Expression of neurofilament (NF) and neuronal nuclei (NeuN)-positive cells surrounding the injury site 6 weeks after TBI. **B, C**: Higher-magnification views of NF and NeuN staining in the cortex around the injury site (**B**) and quantitative analyses of the NF-positive (NF+) area and NeuN-positive (NeuN+) cells (**C**). **D, E**: Higher-magnification views of NF and NeuN staining in CA1, a hippocampal subregion (**D**) and quantitative analyses of the NF-positive (NF+) area and NeuN-positive (NeuN+) cells (**E**). In these images, NF is labeled green, NeuN is red, and nuclei are stained blue. The labels “C” and “H” denote the cortex and hippocampus, respectively. Statistical significance for **D** and **E** was assessed using one-way ANOVA followed by the Tukey correction. * $p < 0.05$; ** $p < 0.01$; *** $p < 0.001$; **** $p < 0.0001$; ns, not significant. All data are expressed as mean \pm standard deviation (SD)

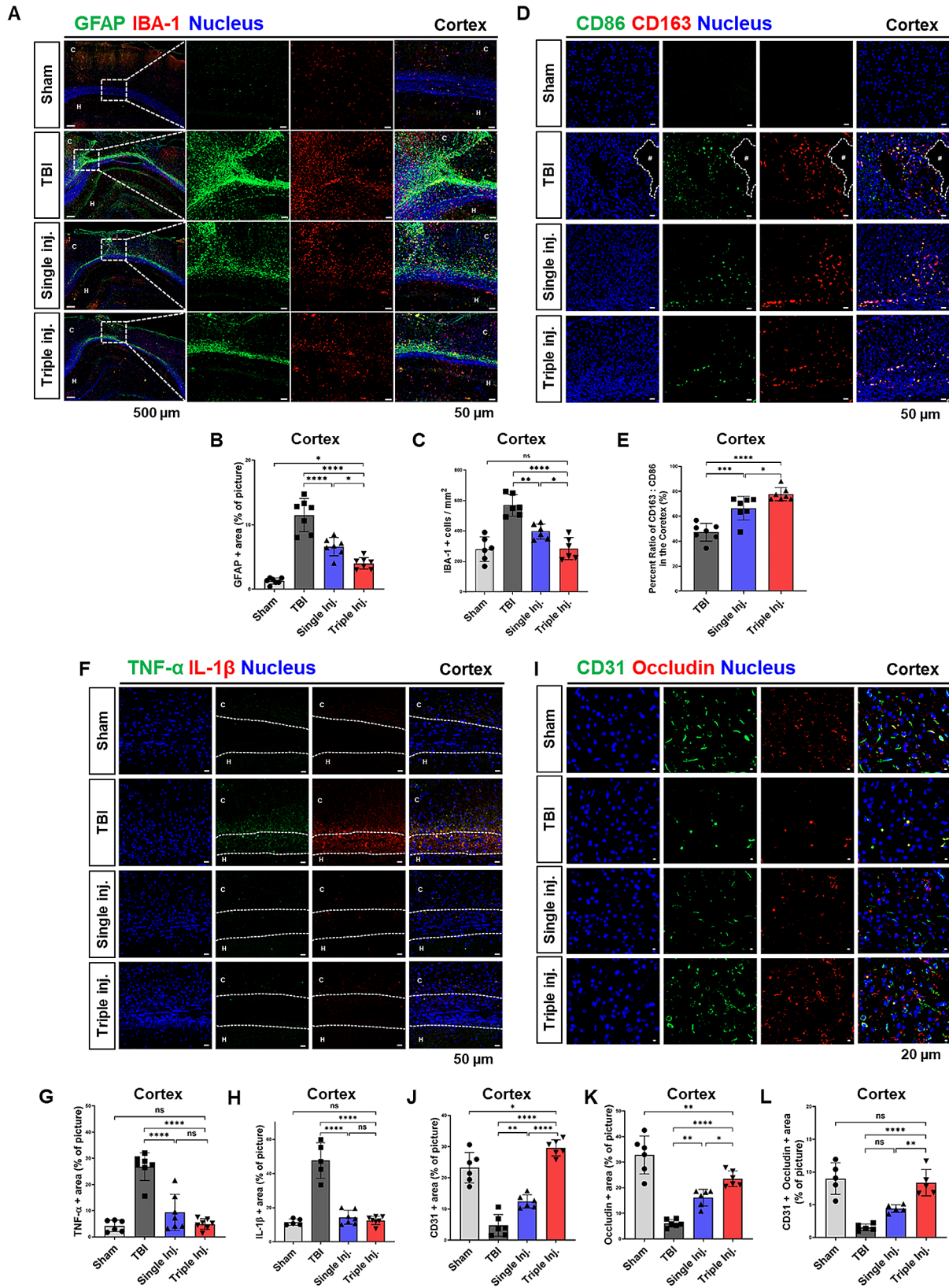


Fig. 7 (See legend on next page.)

(See figure on previous page.)

Fig. 7 Attenuation of inflammatory responses and promotion of functional angiogenesis through repetitive administration of peripheral nerve-derived stem cell (PNSC) spheroids. **A:** Expression of GFAP and IBA-1 around the traumatic brain injury (TBI) site 6 weeks post-injury. **B, C:** Quantitative analysis of the GFAP-positive (GFAP+) area (**B**) and IBA-1-positive (IBA-1+) cells (**C**). GFAP is highlighted in green; IBA-1 in red; nuclei in blue. **"C"** represents the cortex, and **"H"** denotes the hippocampus. **D:** Expression of CD86 and CD163 at the injury site 6 weeks post-TBI. **"#"** marks the lesion cavity. **E:** Quantitative analysis of the CD163 to CD86 ratio. CD86: green; CD163: red; nucleus: Blue. **F:** Expression of tumor necrosis factor alpha (TNF- α) and interleukin-1 β (IL-1 β) around the injury site 6 weeks after TBI. **G, H:** Quantitative analysis of TNF- α -positive (TNF- α +) area (**G**) and IL-1 β -positive (IL-1 β +) area (**H**). TNF- α : green; IL-1 β : red; nucleus: Blue. **C:** cortex, **H:** hippocampus. **I:** Expression of CD31 and Occludin around the injury site 6 weeks post-injury. **J - L:** Quantitative analysis of the CD31-positive (CD31+) area (**J**), Occludin-positive (Occludin+) area (**K**), and the area of co-labeling of CD31 and Occludin (**L**). CD31: green; Occludin: red; nucleus: Blue. Statistical significance for quantitative analyses was determined using one-way ANOVA followed by the Tukey correction. * $p < 0.05$; ** $p < 0.01$; *** $p < 0.001$; **** $p < 0.0001$; ns, not significant. All data are expressed as mean \pm standard deviation (SD)

triple inj. group ($17.45 \pm 1.825\%$) showed a greater degree of recovery than the single inj. group ($14.30 \pm 2.668\%$; $p < 0.05$) (Fig. 6D, E). Neuronal regeneration was significantly greater in the triple inj. group (757.8 ± 95.79) compared to both the TBI group (483.7 ± 85.71 ; $p < 0.001$) and the single inj. group (616.5 ± 52.28 ; $p < 0.05$) near the injury site (Fig. 6B, C). In the CA1 region, neuronal regeneration was notably more extensive in the triple inj. group (352.1 ± 53.54) compared to the TBI group (264.8 ± 57.64 ; $p < 0.05$), although it did not significantly differ from the single inj. group (308 ± 42.65) (Fig. 6D, E). Through the analysis of axonal cytoskeleton (neurofilament) and neuron-specific nuclear protein (NeuN) positive cells, we confirmed that triple injections of PNSC spheroids significantly promoted neuronal regeneration and axonal growth. Notably, axonal regeneration, a critical aspect of neuronal repair, extended to both the cerebral cortex and the CA1 region. The highest expression of mature neuronal nuclei was also noted in these areas.

Mature neurons in the CA1 region were equally visible in H&E images. Analysis of the number of live neurons in the CA1 and CA3 regions demonstrated that the number of living neurons decreased in the TBI group (CA1: 583.3 ± 130.1 , CA3: 281.3 ± 42.39) and was restored by triple injection (CA1: 805.4 ± 134.8 ; $p < 0.05$, CA3: 358.9 ± 34.40 ; $p < 0.01$) of PNSC spheroids (Fig. S2). In addition, as a long-term consequence of TBI, neural stem cells and immature neurons are reduced in number and migration [38]. In terms of neural stem cells allowing neuroregeneration and neuroplasticity in the hippocampal region, many studies described GFAP+Nestin+ cells with radial pyramidal cells in the dentate gyrus (DG) region as type I neural stem cells (glial-like radial neural stem cells) during adult neurogenesis [39]. Therefore, to confirm neurogenesis, we analyzed the ratio of GFAP-positive pyramidal cells (GFAP+ cells/total cells) in the subgranular zone (SGZ) of the DG (Fig. S3). The results indicate that the TBI group (1.362 ± 0.520) had a decreased ratio of GFAP-positive pyramidal cells compared to the sham group (3.933 ± 0.961 ; $p < 0.0001$), and this deficiency was restored by triple intrathecal injections (2.913 ± 0.545 ; $p < 0.001$) of PNSC spheroids.

These results, collectively, demonstrate that triple injection of PNSC spheroids restores adult neurogenesis

and subsequent structural neuroplasticity in the context of TBI, thereby providing an effective strategy for neuronal repair and regeneration and contributing to the recovery of cognitive impairment after traumatic brain injury.

Triple intrathecal injections of PNSC spheroids inhibit glial scarring and inflammatory responses and promote revascularization post-TBI

To ascertain the impact on glial scarring and inflammatory responses, we performed immunofluorescence staining using GFAP, which is a marker of activated astrocytes, and IBA-1 for microglia activation. This approach helps visualize glial scar formation and alterations in microglia that contribute to neuroinflammation after TBI (Fig. 7A). The analysis revealed that PNSC spheroid injections resulted in lower GFAP expression around the injury site than in the TBI group ($11.50 \pm 2.570\%$; $p < 0.0001$), with the triple inj. group ($4.020 \pm 0.891\%$) showing significantly reduced GFAP levels compared to the single inj. group ($6.608 \pm 1.419\%$; $p < 0.05$) (Fig. 7A, B). Similarly, the number of IBA-1 positive cells was significantly lower in the triple inj. group (285.2 ± 72.57) compared to both the TBI group (570 ± 70.51 ; $p < 0.0001$) and the single inj. group (398.2 ± 49.39 ; $p < 0.05$) (Fig. 7A, C). Further, we conducted Sholl analysis to assess the morphological complexity of activated IBA-1-positive microglia (Fig. S4). The analysis revealed fewer branches in the TBI group compared to the sham group, with an increase in branches observed after repeated injections of PNSC spheroids. This showed that the TBI group exhibited a higher proportion of activated amoeboid microglia, whereas the sham and triple injection groups had predominantly resting ramified microglia. Co-immunofluorescence staining with CD86 (M1 marker) and CD163 (M2 marker) was used to evaluate the shift from pro-inflammatory M1 to anti-inflammatory M2 macrophages at 6 weeks post-TBI. The CD163:CD86 ratio was significantly higher in both the single inj. ($66.44 \pm 9.460\%$; $p < 0.001$) and triple inj. groups ($77.67 \pm 5.184\%$; $p < 0.0001$) compared to the TBI group, indicating a shift towards an anti-inflammatory state. The triple inj. group exhibited a higher M2 ratio than the single inj. group (Fig. 7D, E), suggesting enhanced suppression of glial

scarring and neuroinflammation through reduced astrocyte and microglia activation and a shift in macrophage expression. To assess the levels of inflammatory cytokines following TBI, immunofluorescent staining was conducted, co-staining for TNF- α and IL-1 β (Fig. 7F). This analysis revealed significantly elevated TNF- α levels at the glial scar site and in areas with a high density of microglia/macrophages in the TBI group ($26.81 \pm 5.285\%$; $p < 0.0001$) compared to the groups receiving PNSC spheroid injections (Fig. 7E, G). No significant difference was observed between the single inj. group ($9.354 \pm 6.879\%$) and the triple inj. group ($4.906 \pm 2.035\%$) (Fig. 7F, G). Similarly, IL-1 β levels were also significantly higher in the TBI group ($47.57 \pm 10.45\%$; $p < 0.0001$) than in the treatment groups, with no significant difference between the single inj. group ($14.34 \pm 4.071\%$) and the triple inj. group ($12.53 \pm 2.469\%$) (Fig. 7E, H). To assess revascularization at the TBI lesion site following PNSC spheroid injections, immunofluorescence staining was conducted, involving co-labeling with CD31, which is a marker for vascular endothelial cells, and Occludin, which is indicative of tight junctions in the blood-brain barrier (BBB) (Fig. 7I). CD31 expression, denoting the presence of endothelium, was significantly higher in the triple inj. group ($29.59 \pm 2.591\%$) than in the TBI group ($4.719 \pm 3.475\%$; $p < 0.0001$) or the single inj. group ($12.43 \pm 2.122\%$; $p < 0.0001$) (Fig. 7I, J). Similarly, Occludin expression, reflecting BBB integrity, was higher in the triple inj. group ($23.53 \pm 3.064\%$) than in the TBI group ($6.065 \pm 1.500\%$; $p < 0.0001$) and the single inj. group ($16.10 \pm 3.236\%$; $p < 0.05$) (Fig. 7I, K). A further analysis of regions showing co-expression of CD31 and Occludin revealed significantly higher levels in the triple inj. group ($8.385 \pm 2.017\%$) than in the TBI group ($1.546 \pm 0.503\%$; $p < 0.0001$) and single inj. group ($4.414 \pm 0.594\%$; $p < 0.01$), indicating more extensive BBB repair (Fig. 7I, L). These findings suggest that repeated triple injections of PNSC spheroids not only effectively reduce neuroinflammation, but also significantly promote angiogenesis and BBB restoration.

Discussion

In this study, we observed that PNSC spheroids expressed specific markers associated with the Schwann cell lineage, such as GFAP, GAP43, and S100 β . These markers were not present in PNSCs before spheroid formation. Moreover, the formation of spheroids from PNSCs (PNSC spheroids) *in vitro* significantly strengthened their neuroprotective and anti-inflammatory capabilities. Utilizing a rat model of CCI, we found that administering PNSC spheroids via triple intrathecal injections effectively preserved the cerebral cortex from tissue loss, thereby facilitating the recovery of sensorimotor function. Additionally, triple injections of PNSC spheroids diminished

the presence of activated astrocytes and microglial cells and decreased the expression of inflammatory cytokines, indicating a potential to reduce the risk of chronic neuroinflammation. The administration of triple injections of PNSC spheroids within the first week of the acute phase exhibited a more pronounced anti-inflammatory effect than a single injection, and BBB restoration was more effectively achieved with triple injections than with a single dose. In our preceding research, it was demonstrated that PNSC spheroids consistently expressed NC lineage markers, including Nestin, p75NTR, and CD105 [11]. Additionally, NC-specific transcription factors such as Sox2, Sox9, and Sox10 were retained within PNSC spheroids [11]. However, markers associated with the myelin sheath, specifically MBP and MPZ, were not observed in PNSC spheroids [11]. These immunophenotypic characteristics indicate that PNSCs, when aggregated into spheroids, tend to differentiate preferentially towards a Schwann cell lineage, resembling either non-myelinating or dedifferentiated Schwann cells. Overall, PNSC spheroids were found to express and secrete high levels of gli-related neurotrophic mRNAs and factors. This suggests that the neurotrophic potential of PNSCs is enhanced by their organization into 3D spheroids.

The administration of PNSC spheroids via triple intrathecal injections promoted remyelination, axonal regeneration, and the formation of new blood vessels, contributing to the restoration of tissue volume and sensorimotor function, even without scaffolds to facilitate endogenous cell migration. This effect is likely attributable to a range of neurotrophic factors secreted by PNSC spheroids (Fig. 2G-I). Notably, NT-3, encoded by the NTF3 gene, was found to be highly expressed in both PNSCs and PNSC spheroids and is known to exert neuroprotective effects through TrkC receptor-mediated pErk5 activation, as was observed when its recombinant protein was administered in a TBI rat model [40]. PNSC spheroids also exhibited higher expression of GDNF and BDNF than PNSCs alone. These factors are recognized for their significant contributions to neuroprotection and neuroregeneration [41]. Neuroregeneration in the hippocampal region after ischemia-induced brain injury has been emphasized to be highly correlated with the recovery of cognitive function in the brain [42], and it has been suggested that this is possibly related to the increased expression of BDNF in the hippocampal region [43]. In this study, we found an increase in the number of NeuN-positive neurons and live neurons in the hippocampal region after PNSC spheroid injection (Fig. S2) and notably restored adult neurogenesis and subsequent structural neuroplasticity in the SGZ (Fig. S3). This suggests that neurotrophic factor expression and release in PNSC spheroids (Fig. 2G-I) contributes to subsequent cognitive improvement. PNSC spheroids remained detectable in

brain tissue for up to 10 days following the initial injection, but only after triple injections (Fig. S5), indicating that the effects of expression and release of various neurotrophic factors have the potential to be amplified by repeated injections of PNSC spheroids. Therefore, the strategic triple intrathecal injection of PNSC spheroids facilitates neurological functional recovery of injured brain tissue by sustaining elevated levels of neurotrophic factors.

Long-term hyperactivation of astrocytes and microglia can exacerbate neuroinflammation and hinder tissue regeneration by releasing various inflammatory cytokines, contributing to glial scarring, and promoting the recruitment of immune cells [44]. A prior study on spinal cord injuries utilizing PNSC spheroids observed that injecting PNSC spheroids diminished the expression of GFAP, an astrocyte marker, after 8 weeks [11]. Consistent with these earlier findings, our current research also demonstrated a reduction in GFAP expression following PNSC spheroid injections. Moreover, activated astrocytes in the TBI model were identified on both the ipsilateral side and the uninjured contralateral side of the corpus callosum, which links the brain's two hemispheres (Fig. S6). The presence of activated astrocytes on the contralateral side of the corpus callosum, displaying spindle-like morphology, was notably reduced in the group receiving triple injections. This observation suggests that triple injections of PNSC spheroids could potentially mitigate secondary injuries, which are a leading cause of in-hospital fatalities after TBI.

Furthermore, PNSC spheroid injections led to a notable reduction in activated amoeboid microglia, with the highest effect observed after repeated injections. Previous studies have highlighted that chronic neuroinflammation is primarily associated with the presence of activated amoeboid microglia [32, 45]. Consistent with these findings, our data demonstrate that TNF- α and IL-1 β , markers of chronic neuroinflammation, were significantly elevated in the TBI group and reduced in the triple injection group, aligning with the observed changes in microglial branching (Fig. 7F-H). These results suggest that repeated PNSC spheroid injections may mitigate prolonged microglial activation and potentially reduce the risk of long-term neuroinflammation. Although the levels of M1 and M2 macrophages nearly returned to baseline 1-month post-injury (Fig. S7) [46], their densities remained higher in the injury group than in those treated with PNSC spheroid injections. This finding suggests a transitional state of polarized cells (CD86+CD163+ cells) post-TBI. Notably, triple injections of PNSC spheroids diminished macrophage density and increased the CD163/CD86 expression ratio, a key marker of functional recovery after injury [47]. The reduction in the pro-inflammatory cytokines TNF- α

and IL-1 β with repeated PNSC spheroid injections further underscores the decrease in activated astrocytes, microglia, and M1 macrophages [48]. Restoring the BBB is a critical therapeutic goal post-TBI, as its increased permeability can exacerbate neuroinflammation [44]. We observed a significant upregulation of tight junction proteins in the triple injection group, indicating a role for PNSC spheroids in BBB restoration. This study's findings highlight the multifaceted therapeutic benefits of PNSC spheroids for TBI treatment, including neuroprotection, neuroregeneration, anti-inflammation, and angiogenesis.

As the first study on the use of PNSC spheroids in TBI treatment through triple intrathecal injections, it is noteworthy that a recent clinical trial involving intrathecal injections of autologous bone marrow-derived total nucleated cells in children with cerebral palsy has demonstrated the safety of this delivery method [49]. Additionally, a clinical study is ongoing to evaluate the outcomes of subsequent injections after three initial injections of adipose tissue-derived mesenchymal stem cells in TBI patients [NCT02525432]. This preclinical research presents PNSC spheroids as a promising candidate for clinical application in TBI treatment, considering their delivery method, dosage, and effectiveness. Building on our preliminary findings, the next phase of our research involves planning and executing phase 1 clinical trials to explore the safety and impact of PNSC spheroids on various clinical outcomes. We aim to assess the safety profile of PNSC spheroids and their effects on a broad set of clinical parameters. Additionally, the trials will evaluate the effectiveness of repeated intrathecal injections of PNSC spheroids for the treatment of TBI, along with potential long-term advantages of this therapeutic approach for TBI patients.

This study has several acknowledged limitations. Firstly, cognitive assessments specifically related to hippocampal repair were not conducted, despite our analysis of live neurons in the CA1 and CA3 regions. Additionally, confirming the promotion of adult neurogenesis through co-staining with neural progenitor cell markers such as Nestin or Sox2 following repetitive intrathecal injection of PNSC spheroids would be beneficial. Secondly, intrathecal injections can be employed to treat brain lesions or spinal cord lesions, but they carry a risk of arachnoiditis [50, 51]. Moreover, intrathecal injections may have limited capacity to deliver the neurotrophic factors secreted by PNSC spheroids directly to the site of brain injury. Given these limitations, it is advisable to exercise caution when making definitive statements about the repeated safety and effectiveness of this treatment method.

Conclusions

In this study, we explored the therapeutic impact of PNSC spheroids through repeated (triple) intrathecal injections in a rat model of TBI. Our findings indicate that the consistent intrathecal delivery of PNSC spheroids could significantly increase the potential for neurological recovery and tissue regeneration. This method shows great promise in prolonging the therapeutic efficacy of cell products such as PNSC spheroids and amplifying their paracrine effects. Employing functional cellular therapies in conjunction with repeated administrations could represent a pivotal advancement in the treatment of persistent neurological conditions.

Abbreviations

TBI	Traumatic Brain Injury
PNSCs	Peripheral Nerve-derived Stem Cell
CCI	Controlled Cortical Impact
bFGF	Basic Fibroblast Growth Factor
DMEM	Dulbecco's Modified Eagle Medium
NC	Neural Crest
NT-3	NeuroTrophin-3
GDNF	Glial cell-Derived Neurotrophic Factor
EGF	Epidermal Growth Factor
NGF	Nerve Growth Factor
BDNF	Brain-Derived Neurotrophic Factor
CMs	Conditioned Media
BMSCs	Bone Marrow-derived Mesenchymal Stem Cells
TNF- α	Tumor Necrosis Factor- α
IL-1 β	InterLeukin-1 β
mNSS	modified Neurological Severity Score
NTF	Neurotrophin
GAP43	Growth Associated Protein 43
GFAP	Glial Fibrillary Acidic Protein
MPZ	Myelin Protein Zero
NF	Neurofilament
MBP	Myelin Basic Protein
IBA-1	Ionized calcium-Binding Adapter molecule-1

Supplementary Information

The online version contains supplementary material available at <https://doi.org/10.1186/s13287-024-03874-2>.

Supplementary Material 1
 Supplementary Material 2
 Supplementary Material 3
 Supplementary Material 4
 Supplementary Material 5
 Supplementary Material 6
 Supplementary Material 7
 Supplementary Material 8
 Supplementary Material 9
 Supplementary Material 10

Acknowledgements

The authors thank the funders listed in the "Funding" section for their support.

Author contributions

I.H., Y.I.Y. designed the study; K.C., Y.H.H. performed the material development; H.E.S., Y.Y., G.K., E.J.R., B.G.S. and J.H.J. performed the in-vivo experiments. H.E.S., W.J.L., K.S.P., I.H. and Y.I.Y. wrote the paper with input from all authors. All authors have read and agreed to the published version of the manuscript.

Funding

This research was supported by the Korean Fund for Regenerative Medicine (KFRM) grant funded by the Korea government (the Ministry of Science and ICT, the Ministry of Health & Welfare, 21C0717L1), and Basic Science Research Program through the National Research Foundation of Korea (NRF) funded by the Ministry of Education (NRF-2021R111A1A01052791), Republic of Korea. This work was also supported by the 2016 Inje University research grant.

Data availability

Not applicable.

Declarations

Ethics approval and consent to participate

Consent of Committee on the Bioethics and consent to participate: (1) Title of the approved project: Isolation and Cell Banking of Adult Stem Cells Derived from the Myocardium, the Peripheral Nerve, the Skeletal Muscle, Adipose Tissue, and Bone Marrow. (2) Name of the institutional approval committee: The Institutional Review Board (IRB) Committee of Inje University College of Medicine, Republic of Korea. (3) Approval Number: IRB No. 16–0147. (4) Date of approval: September 2nd, 2016. *The donors' guardian provided written informed consent for participation in the study and the use of samples.* The written consent form is provided in the Supplementary Information. Consent of the Committee on the Ethics of Animal Experiments of the Local Ethics Commission: (1) Title of the approved project: Development of regenerative materials for traumatic brain injuries. (2) Name of the institutional approval committee: the Institutional Animal Care and Use Committee (IACUC) of CHA Bundang Medical Center, CHA University, Republic of Korea. (3) Approval Number: IACUC-220189. (4) Date of approval: November 25th, 2022. (1) Title of the approved project: Testing the biodistribution of regenerative medicine for patients with traumatic brain injury. (2) Name of the institutional approval committee: the Institutional Animal Care and Use Committee (IACUC) of CHA Bundang Medical Center, CHA University, Republic of Korea. (3) Approval Number: IACUC230125. (4) Date of approval: July 17th, 2023. The animal studies were conducted according to the ARRIVE guidelines (Animal Research: Reporting of In Vivo Experiments).

Consent for publication

Not applicable.

Competing interests

The authors declare no potential conflict of interest.

Author details

¹Department of Life Science, CHA University School of Medicine, Seongnam-si 13488, Gyeonggi-do, Republic of Korea
²Paik Institute for Clinical Research, Inje University College of Medicine, Busan 47392, Republic of Korea
³Department of Anesthesiology and Pain Medicine, Inje University College of Medicine, Busan 47392, Republic of Korea
⁴Department of Neurosurgery, CHA University, CHA Bundang Medical Center, Seongnam-si 13496, Gyeonggi-do, Republic of Korea
⁵Convergence Stem Cell Therapy Research Team, CHA Future Medical Research Institute, Seongnam 13496, Gyeonggi-do, Korea
⁶Innostem Bio, Busan 47392, Republic of Korea

Received: 22 February 2024 / Accepted: 1 August 2024

Published online: 19 September 2024

References

- Schepici G, Silvestro S, Bramanti P, Mazzon E. Traumatic brain Injury and Stem cells: an overview of clinical trials, the current treatments and future therapeutic approaches. *Med (Kaunas)*. 2020;56(3).

2. Smith DH, Meaney DF, Shull WH. Diffuse axonal injury in head trauma. *J Head Trauma Rehabil.* 2003;18(4):307–16.
3. Andrzejewska A, Dabrowska S, Lukomska B, Janowski M. Mesenchymal stem cells for neurological disorders. *Adv Sci (Weinh).* 2021;8(7):2002944.
4. Kawabori M, Chida D, Nejadnik B, Stonehouse AH, Okonkwo DO. Cell therapies for acute and chronic traumatic brain injury. *Curr Med Res Opin.* 2022;38(12):2183–9.
5. Wang D, Wang S, Zhu Q, Shen Z, Yang G, Chen Y, et al. Prospects for nerve regeneration and Gene Therapy in the treatment of traumatic brain Injury. *J Mol Neurosci.* 2023;73(7–8):578–86.
6. Cox CS Jr., Hetz RA, Liao GP, Aertker BM, Ewing-Cobbs L, Juranek J, et al. Treatment of severe adult traumatic brain Injury using bone marrow mononuclear cells. *Stem Cells.* 2017;35(4):1065–79.
7. Duma C, Kopyov O, Kopyov A, Berman M, Lander E, Elam M, et al. Human intracerebroventricular (ICV) injection of autologous, non-engineered, adipose-derived stromal vascular fraction (ADSVF) for neurodegenerative disorders: results of a 3-year phase 1 study of 113 injections in 31 patients. *Mol Biol Rep.* 2019;46(5):5257–72.
8. Wang S, Cheng H, Dai G, Wang X, Hua R, Liu X, et al. Umbilical cord mesenchymal stem cell transplantation significantly improves neurological function in patients with sequelae of traumatic brain injury. *Brain Res.* 2013;1532:76–84.
9. Kawabori M, Weintraub AH, Imai H, Zinkevych I, McAllister P, Steinberg GK, et al. Cell therapy for chronic TBI: interim analysis of the Randomized Controlled STEMTRA Trial. *Neurology.* 2021;96(8):e1202–14.
10. McCrea MA, Cramer SC, Okonkwo DO, Mattke S, Paadre S, Bates D, et al. Determining minimally clinically important differences for outcome measures in patients with chronic motor deficits secondary to traumatic brain injury. *Expert Rev Neurother.* 2021;21(9):1051–8.
11. Lee HL, Yeum CE, Lee H, Oh J, Kim JT, Lee WJ et al. Peripheral nerve-derived stem cell spheroids induce functional recovery and repair after spinal cord Injury in rodents. *Int J Mol Sci* 2021;22(8).
12. Jeong SY, Lee HL, Wee S, Lee H, Hwang G, Hwang S et al. Co-administration of Resolvin D1 and peripheral nerve-derived stem cell spheroids as a therapeutic strategy in a rat model of spinal cord Injury. *Int J Mol Sci* 2023;24(13).
13. Guha L, Singh N, Kumar H. Different ways to die: cell death pathways and their Association with spinal cord Injury. *Neurospine.* 2023;20(2):430–48.
14. Lee S, Nam H, Joo KM, Lee SH. Advances in neural stem cell therapy for spinal cord Injury: Safety, Efficacy, and future perspectives. *Neurospine.* 2022;19(4):946–60.
15. Kitagawa T, Nagoshi N, Okano H, Nakamura M. A narrative review of advances in neural precursor cell transplantation therapies for spinal cord Injury. *Neurospine.* 2022;19(4):935–45.
16. Ma YH, Liang QY, Ding Y, Han J, Zeng X. Multimodal Repair of spinal cord Injury with mesenchymal stem cells. *Neurospine.* 2022;19(3):616–29.
17. Zhuo Y, Ai K, He K, Wu B, Peng J, Xiang J, et al. Global Research Trends of Exosomes in the Central Nervous System: a bibliometric and visualized analysis. *Neurospine.* 2023;20(2):507–24.
18. Kern S, Eichler H, Stoeve J, Kluter H, Bieback K. Comparative analysis of mesenchymal stem cells from bone marrow, umbilical cord blood, or adipose tissue. *Stem Cells.* 2006;24(5):1294–301.
19. Baudo G, Flinn H, Holcomb M, Tiwari A, Soriano S, Taraballi F et al. Sex-dependent improvement in traumatic brain injury outcomes after liposomal delivery of dexamethasone in mice. *bioRxiv.* 2023.
20. Gupte R, Brooks W, Vukas R, Pierce J, Harris J. Sex differences in traumatic Brain Injury: what we know and what we should know. *J Neurotrauma.* 2019;36(22):3063–91.
21. Weber EM, Dallaire JA, Gaskill BN, Pritchett-Corning KR, Garner JP. Aggression in group-housed laboratory mice: why can't we solve the problem? *Lab Anim (NY).* 2017;46(4):157–61.
22. Ni H, Rui Q, Kan X, Gao R, Zhang L, Zhang B. Catalpol ameliorates oxidative stress and neuroinflammation after traumatic brain Injury in rats. *Neurochem Res.* 2023;48(2):681–95.
23. Jensen MB, Krishnaney-Davison R, Cohen LK, Zhang SC. Injected versus oral cyclosporine for human neural progenitor grafting in rats. *J Stem Cell Res Ther* 2012;Suppl 10:003.
24. Chen J, Sanberg PR, Li Y, Wang L, Lu M, Willing AE, et al. Intravenous administration of human umbilical cord blood reduces behavioral deficits after stroke in rats. *Stroke.* 2001;32(11):2682–8.
25. Cho DY, Jeun SS. Combination therapy of human bone marrow-derived mesenchymal stem cells and minocycline improves neuronal function in a rat middle cerebral artery occlusion model. *Stem Cell Res Ther.* 2018;9(1):309.
26. Antonova VV, Silachev DN, Ryzhkov IA, Lapin KN, Kalabushev SN, Ostrova IV et al. Three-hour argon inhalation has no neuroprotective effect after Open Traumatic Brain Injury in rats. *Brain Sci.* 2022;12(7).
27. Ehltling A, Zweyer M, Maes E, Schleeuber Y, Doshi H, Sabir H et al. Impact of Hypoxia-Ischemia on Neurogenesis and Structural and Functional outcomes in a mild-moderate neonatal hypoxia-ischemia brain Injury Model. *Life (Basel).* 2022;12(8).
28. Wu Q, Wang H. The spatiotemporal expression changes of CB2R in the hippocampus of rats following pilocarpine-induced status epilepticus. *Epilepsy Res.* 2018;148:8–16.
29. Donat CK, Yanez Lopez M, Sastre M, Baxan N, Goldfinger M, Seemamber R, et al. From biomechanics to pathology: predicting axonal injury from patterns of strain after traumatic brain injury. *Brain.* 2021;144(1):70–91.
30. Kim S, Nam Y, Kim C, Lee H, Hong S, Kim HS et al. Neuroprotective and Anti-inflammatory Effects of Low-Moderate Dose Ionizing Radiation in Models of Alzheimer's Disease. *Int J Mol Sci* 2020;21(10).
31. Roh EJ, Kim DS, Kim JH, Lim CS, Choi H, Kwon SY, et al. Multimodal therapy strategy based on a bioactive hydrogel for repair of spinal cord injury. *Biomaterials.* 2023;299:122160.
32. Liu Q, Wang Z, Cao J, Dong Y, Chen Y. Dim Blue Light at Night Induces Spatial Memory Impairment in Mice by Hippocampal Neuroinflammation and Oxidative Stress. *Antioxidants (Basel).* 2022;11(7).
33. Alam A, Thelin EP, Tajsic T, Khan DZ, Khellaf A, Patani R, et al. Cellular infiltration in traumatic brain injury. *J Neuroinflammation.* 2020;17(1):328.
34. O'Carroll SJ, Kho DT, Wiltshire R, Nelson V, Rotimi O, Johnson R, et al. Pro-inflammatory TNFalpha and IL-1beta differentially regulate the inflammatory phenotype of brain microvascular endothelial cells. *J Neuroinflammation.* 2015;12:131.
35. Choi B, Lee C, Yu JW. Distinctive role of inflammation in tissue repair and regeneration. *Arch Pharm Res.* 2023;46(2):78–89.
36. Hinkley LB, Marco EJ, Findlay AM, Honma S, Jeremy RJ, Strominger Z, et al. The role of corpus callosum development in functional connectivity and cognitive processing. *PLoS ONE.* 2012;7(8):e39804.
37. Bartsch T, Dohring J, Rohr A, Jansen O, Deuschl G. CA1 neurons in the human hippocampus are critical for autobiographical memory, mental time travel, and autozoetic consciousness. *Proc Natl Acad Sci U S A.* 2011;108(42):17562–7.
38. Ibrahim S, Hu W, Wang X, Gao X, He C, Chen J. Traumatic brain Injury causes aberrant Migration of Adult-born neurons in the Hippocampus. *Sci Rep.* 2016;6:21793.
39. Nicola Z, Fabel K, Kempermann G. Development of the adult neurogenic niche in the hippocampus of mice. *Front Neuroanat.* 2015;9:53.
40. Akyol O, Sherchan P, Yilmaz G, Reis C, Ho WM, Wang Y, et al. Neurotrophin-3 provides neuroprotection via TrkC receptor dependent pErk5 activation in a rat surgical brain injury model. *Exp Neurol.* 2018;307:82–9.
41. Mishchenko TA, Klimenko MO, Kuznetsova AI, Yarkov RS, Savelyev AG, Sochilina AV, et al. 3D-printed hyaluronic acid hydrogel scaffolds impregnated with neurotrophic factors (BDNF, GDNF) for post-traumatic brain tissue reconstruction. *Front Bioeng Biotechnol.* 2022;10:895406.
42. Bendel O, Bueters T, von Euler M, Ove Ogren S, Sandin J, von Euler G. Reappearance of hippocampal CA1 neurons after ischemia is associated with recovery of learning and memory. *J Cereb Blood Flow Metab.* 2005;25(12):1586–95.
43. Sayyah M, Seydousefi M, Moghanlou AE, Metz GAS, Shamsaei N, Faghfoori MH, et al. Activation of BDNF- and VEGF-mediated neuroprotection by Treadmill Exercise Training in Experimental Stroke. *Metab Brain Dis.* 2022;37(6):1843–53.
44. Bai Q, Xue M, Yong VW. Microglia and macrophage phenotypes in intracerebral haemorrhage injury: therapeutic opportunities. *Brain.* 2020;143(5):1297–314.
45. Caplan HW, Cardenas F, Gudenkauf F, Zelnick P, Xue H, Cox CS, et al. Spatio-temporal distribution of Microglia after Traumatic Brain Injury in male mice. *ASN Neuro.* 2020;12:1759091420911770.
46. Turtzo LC, Lescher J, Janes L, Dean DD, Budde MD, Frank JA. Macrophagic and microglial responses after focal traumatic brain injury in the female rat. *J Neuroinflammation.* 2014;11:82.
47. Peruzzaro ST, Andrews MMM, Al-Gharibeh A, Pupiec O, Resk M, Story D, et al. Transplantation of mesenchymal stem cells genetically engineered to overexpress interleukin-10 promotes alternative inflammatory response in rat model of traumatic brain injury. *J Neuroinflammation.* 2019;16(1):2.

48. Jurga AM, Paleczna M, Kuter KZ. Overview of General and discriminating markers of Differential Microglia phenotypes. *Front Cell Neurosci.* 2020;14:198.
49. Mancias-Guerra C, Marroquin-Escamilla AR, Gonzalez-Llano O, Villarreal-Martinez L, Jaime-Perez JC, Garcia-Rodriguez F, et al. Safety and tolerability of intrathecal delivery of autologous bone marrow nucleated cells in children with cerebral palsy: an open-label phase I trial. *Cytotherapy.* 2014;16(6):810–20.
50. Singer W, Dietz AB, Zeller AD, Gehrking TL, Schmelzer JD, Schmeichel AM, et al. Intrathecal administration of autologous mesenchymal stem cells in multiple system atrophy. *Neurology.* 2019;93(1):e77–87.
51. Madhavan AA, Summerfield D, Hunt CH, Kim DK, Krecke KN, Raghunathan A, et al. Polyclonal lymphocytic infiltrate with arachnoiditis resulting from intrathecal stem cell transplantation. *Neuroradiol J.* 2020;33(2):174–8.

Publisher's Note

Springer Nature remains neutral with regard to jurisdictional claims in published maps and institutional affiliations.